Universidade de Lisboa
Faculdade de Ciências
Departamento de Biologia Vegetal

Role of Arl13b-exocyst interaction in ciliogenesis

Hugo António Fragoso Moreiras

Dissertação

Mestrado em Biologia Molecular e Genética

2014

Universidade de Lisboa
Faculdade de Ciências
Departamento de Biologia Vegetal

Role of Arl13b-exocyst interaction in ciliogenesis

Hugo António Fragoso Moreiras

Dissertação

Mestrado em Biologia Molecular e Genética

Sob a orientação científica de:

- Dr. Duarte Barral

(Professor Auxiliar da Faculdade de Ciências Médicas da Universidade Nova de Lisboa; *Principal Investigator* no *Membrane traffic in Infection and Disease Group* do Centro de Estudos de Doenças Crónicas-CEDOC)

- Professora Dra. Rita Zilhão

(Professor Associado do Departamento de Biologia Vegetal da Faculdade de Ciências da Universidade de Lisboa)

Mestrado em Biologia Molecular e Genética

2014

Acknowledgements

I would like to express my gratitude to my supervisor, Dr. Duarte Barral, whose expertise and knowledge in many areas contributed considerably in the development of my master thesis in *Membrane Traffic in Infection and Disease* lab.

I would like to thank Dra. Rita Zilhão from Faculdade de Ciências da Universidade de Lisboa for her constant support and interest showed in my work during the past year.

A special thanks also to Dra. Cecília Seixas, who taught me to think and work as a scientist. Without her teaching, patience and support during my period in the lab this thesis would not have been possible.

I also want to leave a special word for Ana Portelinha, Carolina Matos, Cristina Casalou, Cristina Escrevente, Elsa Seixas, Francisco Pereira, Lilia Espada, Maria Serrano, Margarida Correia, Nuno Claudio and Remy Cardoso. You help me to growth as a scientist and as a person and I am very grateful to had the change to meet you all and work and learn with you. And off course I would never forget the incredible moments we spend together in the lab and in all the activities we made together.

I would like also to acknowledge Dra. Susana Lopes form Cilia Regulation & Disease lab for the opportunity she gave me to work with zebrafish in her lab. I also would like to thank Pedro Sampaio and Petra Pintado, as well as the other members of the group, for teaching me the tecnhiques and helping me in the interpretation of the results. I would like to thank all the staff of the fish-facility for all the help and support.

To all my colleagues in CEDOC with whom I share great moments and were always there for support and motivation. Without the amazing team that this institution provides from the researchers until the managing office every step of this journey would have been more difficult. I wish you all the best luck in your life and that we could work together in the future.

I like to thank my friends from the University and from my hometown that directly or indirectly, help and support me during the last years leading to this moment.

Finally, I want to thank my parents and my brother for the unconditional support. Without you I will never be here and will never become the person I am today. You know I love you with all my heart and that my biggest goal in life is to always see you proud.

Table of Contents

List of Figures

Resumo Alargado

Os cílios primários são organelos sensoriais expostos à superfície da maioria das células eucarióticas. Estes funcionam como estruturas semelhantes a antenas, detectando e transmitindo sinais químicos provenientes do ambiente extracelular para o interior da célula. A sua correcta formação e funções sensoriais são fundamentais para o adequado desenvolvimento embrionário e pós-natal, bem como para a homeostase dos tecidos no adulto. De facto, diversas doenças humanas, conhecidas por ciliopatias, devem-se a defeitos no cílio primário. Este organelo é constituído por um axonema que se forma a partir do corpo basal, originado pelo centríolo-materno da célula, e uma membrana ciliar que encerra uma pequena porção do citoplasma designado por ciliopasma. A membrana ciliar e a membrana plasmática são topologicamente contínuas mas diferem na sua composição lipídica. A membrana ciliar contém vários receptores de sinalização celular, canais iónicos e proteínas de transporte que tornam este organelo numa autêntica antena celular.

Até ao momento, ainda não é totalmente conhecido o conjunto de proteínas que regula o processo de montagem do cílio. Várias pequenas proteínas G da superfamília Ras foram implicadas neste processo. Estas proteínas são conhecidas por regularem as vias de tráfego intracelular, assegurando o transporte correcto de moléculas entre compartimentos delimitados por membranas. O cílio primário é um desses compartimentos, e é sabido que as proteínas ciliares são transportadas do citoplasma até ao cílio através destas vias de tráfego intracelular, uma vez que este organelo não possui maquinaria para realizar a síntese proteica. Em particular, proteínas da família “Arf-like” (Arl) tais como a Arl3, Arl6 e Arl13b foram associadas ao cílio primário. Mutações nestas proteínas causam distrofia e disfunção renal, obesidade, polidactilia, entre outros defeitos característicos de ciliopatias.

O nosso grupo descobriu recentemente que a Arl13b tem um papel na regulação de tráfego endocítico de reciclagem. Por outro lado, mutações do gene que codifica a Arl13b provocam síndrome de Joubert, uma ciliopatia caracterizada por defeitos neurológicos. Em ratinhos, a mutação de Arl13b causa letalidade embrionária devido a falhas na via de sinalização “Sonic Hedgehog”, presumivelmente causadas por anomalias na estrutura dos cílios primários. Dado que uma das vias que as proteínas ciliares utilizam para chegar ao cílio depende do tráfego endocítico de reciclagem, os nossos resultados que sugerem um papel da Arl13b na regulação desta via poderão contribuir para explicar os defeitos no cílio primário que advêm de mutações na Arl13b. Sendo assim, é possível que a Arl13b tenha um papel no endereçamento/ancoragem de vesículas endocíticas de reciclagem, transportando proteínas ciliares para a região periciliar.

Para além disso, é sabido que as proteínas G quando estão no seu estado activo ou ligadas a GTP efectuam as suas funções ligando-se a proteínas designadas por efectores. O nosso grupo obteve evidências sólidas de que Arl13b interage com o exocisto, através da sua subunidade Sec8. O exocisto é um complexo formado por oito subunidades que participa na ligação e ancoragem de vesículas provenientes da rede trans-Golgi e do compartimento endocítico de reciclagem. Recentemente, a subunidade Exo84 do exocisto foi identificada como mutada em pacientes de síndrome de Joubert e através da subunidade Sec10 foi comprovado que o exocisto está envolvido na formação de cílios. Sendo assim, colocámos como hipótese que o papel da Arl13b no tráfego de proteínas ciliares para a região periciliar ocorra através da sua interação com o exocisto.

Desta forma, o nosso objectivo é estudar o papel da interacção entre Arl13b e o exocisto na ciliogénese e no tráfego ciliar. O nosso primeiro objectivo foca-se na caracterização da interação entre Arl13b e Sec8. O segundo objectivo concentra-se no papel da interação Arl13b-exocisto na formação de cílios.

Os nossos resultados provam que o Sec8 é uma efector da Arl13b, uma vez que a ligação entre as proteínas aumenta na presença de GTP, em linhas celulares de mamífero e que esta interação é independente da presença de cílio. Mostramos também através da síntese *in vitro* de Arl13b-FLAG e Sec8-Myc que a interação entre estas proteínas é directa e que não necessita da presença das outras subunidades do complexo. Para além disso, observamos também que tanto o domínio N-terminal como o C-terminal da Arl13b são necessários para garantir que esta interação ocorra, uma vez que o domínio N-terminal é responsável pela ligação ao efector e o domínio C-terminal é responsável por estabilizar a proteína e garantir a alteração entre a forma activa e inactiva da mesma garantido a troca entre GTP e GDP. São necessários mais estudos para determinar que região da Arl13b é responsável pela viabilidade da interação com o exocisto, sendo para isso necessário produzir novos plasmídeos de Arl13b com deleções mais pequenas e com mutações pontuais para que a conformação da proteína quando expressa nas células não sofra alterações tão drástica e seja possível determinar a região de interação. Vimos também que outra subunidade do exocisto, o Exo70, é co-immunoprecipitada com Arl13b. Este resultado levanta uma nova hipótese em que o Sec8 medeia a interação entre a Arl13b e todo o complexo exocisto. Por ultimo, mostramos também pela primeira vez que o Sec8 é necessário para a correta ciliogénese, uma vez que ao silenciarmos o Sec8 obtemos uma redução na percentagem de células ciliadas . Este fenótipo não é tão acentuado como o observado aquando do silenciamento da Arl13b mas permite especular que as duas proteínas possam estar envolvidas na mesma via de transporte de proteínas necessárias

para a correta formação do cílio. Este resultado reforça a ideia de que a Arl13b é uma peça chave na formação e manutenção da correta biologia ciliar.

Um colaborador deste projeto observou uma interação genética sinérgica entre a Arl13b e Sec10 indicando que estas proteínas participam num via comum ou paralela. Em conclusão, com os resultados apresentados neste trabalho, com as informações obtidas a partir do nosso colaborador e com o facto de que Arl13b regula o tráfego endocítico de reciclagem, nós propomos um modelo onde a Arl13b e o exocisto estão envolvidas no transporte de proteínas ciliares originárias do compartimento endocítico de reciclagem até ao interior do cílio. No nosso modelo, o processo baseia- se em dois passos: o Sec8 numa primeira fase é responsável pela seleção e transporte de vesículas contendo Arl13b até à região periciliar; numa segunda fase Exo70 é responsável pela fusão dessas vesículas com a membrana ciliar permitindo a libertação das proteínas ciliares no cilioplasma.

Mais estudos são necessários para testar esta hipótese e comprovar o modelo proposto. Os resultados aqui apresentados e os estudos futuros propostos irão fornecer a base para melhor compreender e interpretar a pleiotropia fenotípica e etiologia do síndrome de Joubert.

Palavras-chave: Cílio, Arl13b, exocisto, imunoprecipitação, ciliogénese, tráfego vesicular, pequenas proteínas G, ciliopatias e síndrome de Joubert.

Abstract

Primary cilia are sensory organelles present on nearly every eukaryotic cell. Arl13b belongs to the Arf family of small G proteins. Mutations in this protein were identified in patients with Joubert syndrome, a ciliopathy characterized by neurological defects combined with polydactyly and cystic kidneys. Nevertheless, the precise role of Arl13b in ciliogenesis remains elusive.

We found that Sec8, a subunit of the exocyst, interacts with Arl13b. The exocyst is an octameric complex involved in the tethering of post-Golgi vesicles at their site of fusion, and it has been shown to be required for cilia formation. Interestingly, it was identified in a family with Joubert syndrome amutation in one of the subunit of the exocyst. Furthermore we show that Sec8 is a *bona fide* effector of Arl13b, since it binds only to the activated form of Arl13b, and that the interaction is direct. We proved that both the N- and C- terminal of Arl13b are required for the interaction with Sec8. Moreover, we found that Exo70, another subunit of the exocyst, also co-immunoprecipitates with Arl13b, suggesting that Sec8 mediates the interaction of Arl13b with the exocyst complex. Regarding the ciliogenesis defects, we show for the first time that silencing of Sec8 causes an abrogation in cilia formationTogether, these results suggest that Arl13b and exocyst function together in the same pathway during cilia-related processes leading to functional cilia. Since we and others found that Arl13b are involved in endocytic recycling trafficking form the endocytic recycling compartment, it is possible that both proteins work together in the transport of recycling vesicles containing ciliary proteins from the endocytic recycling compartment toward primary cilia.

Keywords: Cilia, Arl13b, exocyst, immunoprecipitation, ciliogenesis, vesicular trafficking, small G proteins, ciliopathies and Joubert syndrome.

Abbreviations

5-HTR6 – 5-Hydroxytryptamine receptor 6

ADPKD – Autossomal dominant polycystic kidney disease

AMPA - α-amino-3-hydroxy-5-methyl-4-isoxazolepropionic acid

BBS – Bardet-Biedl syndrome

BCS – Bovine calf serum

COPI and COPII – Coat Protein Complex I and II

CTS- Ciliary targeting signals

DMEM – Dulbecco's modified eagle's medium

DMEM/F-12 - Dulbecco's modified eagle's medium/nutrient mixture

DTT – Dithiothreitol

EE – Early endosomes

ER – Endoplasmic reticulum

ERC – Endocytic recycling compartment

FBS – Fetal bovine serum

FRAP – Fluorescence recovery after photobleaching

GAP – GTPase-activating proteins

GAPDH – Glyceraldehyde-3-phosphate dehydrogenase

GDP – Guanosine diphosphate

GEF – Guanine nucleotide exchange factors

GPCR – G-protein-coupled receptors

G proteins – GTP-binding proteins

GTP – Guanosine triphosphate

IFT – Intraflagellar transport

IMCD3 – Inner medullary collecting duct

JBTS – Joubert syndrome

KV – Kupffer's vesicle

LE – Late endosomes

MDCK – Mardin-Darby canine kidney

MKS – Meckel-Gruber syndrome

MO – Morpholino

NPHP – Nephronophtisis

PDGF – Platelet-derived Growth Factor

PKD1 – Polycystin 1

PKD2 – Polycystin 2

PM – Plasma membrane

qRT-PCR – Quantitative real-time polymerase chain reaction

RT – Room temperature

siRNA – Small interfering RNA

Shh – Sonic Hedgehog

Smo – Smoothened

SSTR3 – somatostatin receptor 3

TGN – Trans-Golgi network

TNT – Transcription and translation

TZ – Transition Zone

Wnt – Wingless-int

1 Introduction

1.1 Types of cilia

Cilia are primordial eukaryotic structures, present on the surface of most mammalian cell types. These antenna-like projections are known to be essential for several signalling cascades, such as Sonic Hedgehog (Shh), Wingless-int (Wnt), Platelet-derived Growth Factor (PDGF) and Hippo (*1*–*3*).

Cilia are composed by an axoneme that extends from a basal body, is derived from the mother centriole and a ciliary membrane that encloses a small fraction of the cell cytoplasm called the cilioplasm (Figure 1). The ciliary membrane contains several signalling receptors, ion channels and transport proteins, as well as some of their downstream effectors (*2*, *4*, *5*). The ciliary and plasma membranes are topologically continuous but differ in their lipoprotein composition (*1*, *3*, *6*, *7*). Several important structures localize to the base of the cilium: the ciliary pocket, an invagination found at the junction of the plasma membrane and the ciliary membrane where clathrin-coat pits and vesicles accumulate; the septin ring, transition fibers, and the transition zone (*3*, *5*).

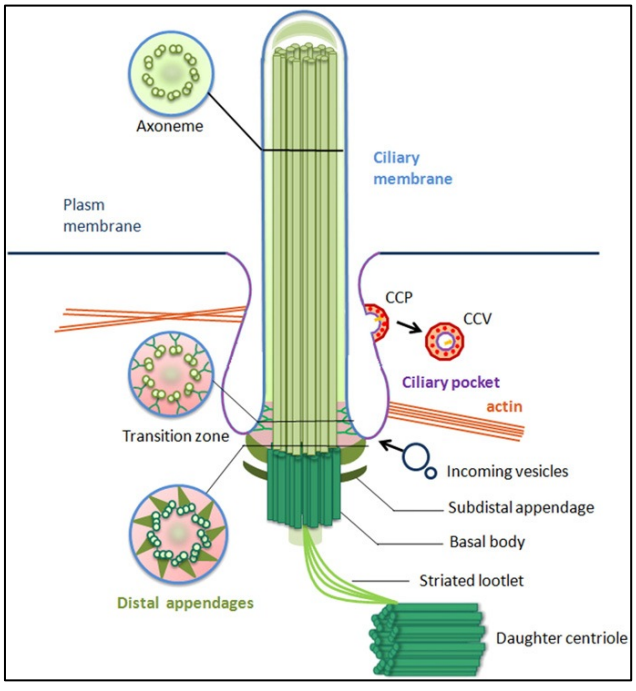

Figure 1 – Primary cilia structure. Schematic representation of the structure of the primary cilium showing the basal body, axoneme, ciliary membrane, transition zone and ciliary pocket with clathrin-coated pits (CCP) and clathrin-coated vesicles (CCV) formation. Taken from Ke *et al*, 2014 (*3*).

Cilia can be classified into two main categories: motile and primary. The axoneme of motile cilia consists of a set of 9 microtubules doublets with a microtubule central pair, usually referred to as a "9+2" structure (*1*–*3*). In contrast, the axoneme of primary cilia consists in a "9+0" structure, without a central pair (*1*, *2*, *8*). Additionally, motile cilia are usually longer than primary cilia, which typically have 5–10 µm in length (*8*).

Motile cilia are usually present in multiple copies and can be found in respiratory epithelia, oviduct, brain ventricles and sperm (*2*, *9*). They bend in a sine-wave fashion to generate fluid movement or cell propulsion, regulating embryonic left-right patterning, clearing airway mucus and generating in cerebrospinal fluid movement (*1*, *10*, *11*).

Primary cilia are usually present in a single copy per cell and can be found in epithelial and endothelial cells, connective tissues and muscle cells as well as neurons (*2*, *9*). By being involved in several signalling cascades they regulate processes such as embryogenesis, tumorigenesis, tissue homeostasis, cell migration, differentiation, cell division, and apoptosis, as well as kidney function, vision and smell (*2*, *9*, *11*).

Furthermore, primary cilia present in the node are motile and generate a fluid flow responsible for defining the left-right patterning during organogenesis. Thus, they can be considered a third group of cilia, the nodal cilia (*8*, *12*).

1.1.1 Ciliary structure

Ciliogenesis is triggered when the centrosome migrates towards the cell surface during the G0 and G1 phases of the cell cycle. The mother and daughter centrioles of the basal body are connected by 2–4 striated rootlets and consist of 9 sets of triplet microtubules, designated A, B, and C and named according to the distance from the center of the centrosome (*1*, *3*).

When the mother centriole migrates to the cell membrane, it anchors to the plasma membrane and then differentiates into the basal body of the primary cilium. The A and B microtubules protrude from the cell surface to form the axoneme and C microtubules terminate before the axoneme starts at a region known as the transition zone (TZ) (*1*, *3*, *9*).

The TZ is found just above the basal body and is essential for the regulation of ciliary protein composition. The microtubule doublets at the TZ are attached to the ciliary membrane by Y-shaped links, forming a membrane specialization called the ciliary necklace (*3*, *5*, *9*). The TZ is formed by transition fibers and a septin ring that function together to provide a large docking site around the base of the cilium for vesicles and protein complexes. Importantly, the TZ prevents the exchange of material between the cytoplasm and the axoneme. This is achieved due to a nine-bladed propeller-like structure with a 60 nm space

between two consecutives sheets, known as the distal appendages where, in theory, large protein complexes can fit but not vesicles. Thus, the TZ serves as a diffusion barrier, through which only selected proteins are allowed to pass into the cilium (*1*, *5*, *13*, *14*).

As referred previously, the internal structure of primary cilia is composed by the axoneme, the core of these organelles. The axoneme consists of a complete A-microtubule, composed by 13 parallel protofilaments, and an adjacent incomplete B-microtubule, composed by 10 protofilaments. Each protofilament is formed by the polymerization of α- and β-tubulin heterodimers from the base to the distal tip of the cilia (*1*, *15*).

Several post-translational modifications are required in order to establish functional axoneme microtubules, including acetylation, palmitoylation, tyrosination/detyrosination, glutamylation, and glycosylation. Microtubule acetylation is the most frequent post-translational modification and has been associated with cilia stabilization (*3*, *16*, *17*). Indeed, acetylated tubulin staining is commonly used to identify cilia.

1.1.2 Ciliary membrane

Primary cilia emerge from the cell membrane by two different ways: one is based on the direct protrusion of cilia from the membrane into the extracellular milieu upon anchoring of the basal body to the cell membrane; the second establishes that primary cilia are partially buried intracellularly and emanate from a membrane invagination termed the ciliary pocket (*3*). This membrane domain is associated with clathrin-coated pits and vesicles, indicating that this is an active site for vesicular trafficking and endocytosis (*3*, *14*).

The ciliary membrane is known to be enriched in several signalling receptors like the G-protein-coupled receptors (GPCRs), which consist of a single polypeptide that is folded into a globular shape and polycystins that function as a Ca^{2+}-permeable cation channel, and are only present in cilia. Phosphatidylinositol-4-phosphate adaptor protein-2 (FAPP2) was shown to be involved in the transport of lipidrafts, a component of the diffusion barrier that controls differences in protein content between the ciliary and plasma membranes. Furthermore, FAPP2 is necessary for ciliogenesis and when depleted leads to an accumulation of vesicles in the basal body region, suggesting that lipidrafts are necessary for ciliary transport and consequently cilia formation (*6*, *11*, *13*, *18*).

1.2 Vesicular trafficking

Vesicular transport involves the budding of a vesicle containing sorted cargo from a donor compartment; movement of the vesicular carrier via cytoskeletal filaments such as microtubules and/or actin towards a target compartment; tethering and docking of the vesicle

with the target compartment membrane in a close physical association; and finally fusion of the carrier with the acceptor compartment, releasing the cargo into the lumen of the target compartment (*19*, *20*).

Vesicular trafficking pathways are usually separated into two main routes: a) the secretory pathway starting at the endoplasmic reticulum (ER) and ending at the plasma membrane (PM), passing through the Golgi apparatus; and b) the endocytic pathway from the PM to lysosomes, through early and late endosomes (EE, LE). Anterograde and retrograde routes between the trans-Golgi network (TGN) and endosomes connect both pathways. Through the endocytic pathway cells internalize extracellular material, ligands and plasma membrane proteins and lipids. The endocytic recycling pathway is also responsible for controlling the composition of the plasma membrane. After endocytosis, cargo is delivered to the early/sorting endosome from where it can be recycled to the PM by a fast recycling pathway, or sorted to the endocytic recycling compartment (ERC) to follow a slow recycling route from the ERC to the plasma membrane. Cargo that is not recycled is routed to late endosomes and lysosomes for degradation or to the TGN (*21*, *22*). Endocytic recycling pathways are important for a wide range of processes like cell migration (*23*) and ciliogenesis (*24*).

Eukaryotic cells have evolved strategies to transfer cargo between different membrane-bound compartments in a specific and regulated manner. This allows them to display a spatial and temporal organization of many cellular processes that is controlled by small GTP-binding proteins (G proteins) of the Ras superfamily, among others. Each step of vesicular trafficking requires a specific set of regulatory molecules. Vesicle budding and cargo selection involve the recruitment of large multi-subunit protein complexes, termed coats, such as clathrin or Coat Protein Complexes I and II (COPI and COPII) (*25*, *26*). After the vesicles pinch off the donor compartment, they are uncoated and transported along microtubules and/or actin filaments, propelled by motor proteins. Kinesin motors guide the anterograde transport of vesicles, from the center of the cell towards the periphery, to the microtubules plus-ends. In contrast, dynein motors guide the retrograde transport towards the microtubules minus-ends (*21*). Tethering/docking of vesicles to acceptor compartments is regulated by tethering protein complexes like the exocyst, the conserved oligomeric Golgi (COG) and the Golgi-associated retrograde proteins (GRAP) (*27*). Finally, fusion of the vesicle with the acceptor compartment membrane is mediated by proteins called SNAREs (soluble N-ethylmaleimide-sensitive factor activating protein receptor) (*28*, *29*). These integral membrane proteins can be classified as vesicular (v-) or target (t-) SNAREs, according to their localization, in the transport vesicle or in the target membrane, respectively (*30*). Importantly, the correct transport between intracellular compartments is ensured through a combination of these molecular players. Moreover, these proteins localize

specifically to different intracellular compartments and are commonly used as markers that allow their identification.

1.2.1 Small G proteins

Structurally, all small G proteins are characterized by four conserved domains for guanine nucleotide binding and GTPase activities and a domain for interaction with downstream effectors (*20*, *31*, *32*). The Ras superfamily of small G proteins can be divided into five different major families: Ras (Ras sarcoma), Rho (Ras homologous), Ran (Ras-like nuclear), Rab (Ras-like in the brain), and Arf (ADP-ribosylation factor) (*31–34*).

The Arf family includes Arl (Arf-like), Arp (Arf-related proteins) and Sar (Secretion-associated and Ras-related) proteins that are involved in vesicle formation at the Golgi and regulation of membrane traffic through the recycling pathways regulation and also in cytoskeleton rearrangement (*32*, *34*, *35*).

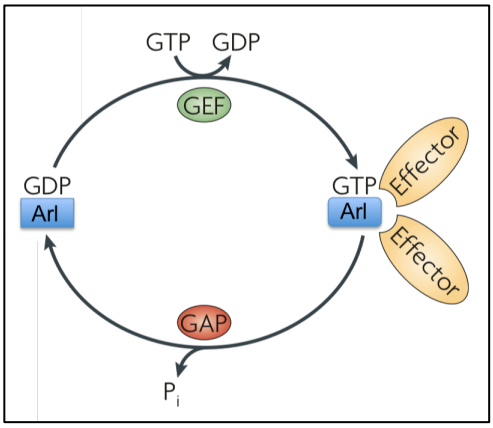

Figure 2 – Arl small G proteins function as molecular switches. Exchange of GDP for GTP is catalyzed by guanine nucleotide exchange factors (GEF), leading to a conformational change. The active conformation is recognized by effector proteins and is converted to the inactive form through GTP hydrolysis, catalyzed by a GTPase-activating protein (GAP). Taken from Stenmark 2009 (*20*).

Small G proteins function as molecular switches that alternate between two conformational states: the guanosine triphosphate (GTP)-bound or active state, and the guanosine diphosphate (GDP)-bound or inactive form (Figure 2) (*20*, *32*, *34*). When activated, small G proteins suffer conformational changes in switch I and switch II regions that allow effector binding (*20*, *36*). Besides these changes, Arf family proteins suffer an additional conformational change in the N-terminal region, allowing these proteins to interact with membranes when in their active state (*34*, *35*).

Conversion of GDP-bound state to GTP-bound state is catalyzed by guanine nucleotide exchange factors (GEFs) that recognise specific residues in the switch regions

and favour the GDP release. This is considered a rate-limiting step since the GEF need to be activated by an upstream signal to catalyze this reaction. The switch occurs when GTP binds to the protein, immediately after GDP has been released. On the other hand, the conversion of the GTP-bound to the GDP-bound form occurs in a faster way, since the GTP is hydrolyzed by the GTPase intrinsic activity that most of these proteins possess and is also facilitated by the catalytic activity of GTPase-activating proteins (GAPs), leading to the release of the downstream effectors. Thus, with this cycle of activation and inactivation, small G proteins transduce an upstream signal to a downstream effector (*19*, *20*, *32*, *34*).

1.2.2 Arl proteins and ciliogenesis

Several small G proteins have been shown to be involved in cilia formation and function. In particular, three members of the Arl subfamily, have been associated with ciliogenesis and cilia signalling (*37*). Arl3 was found to negatively regulate ciliogenesis (*38*). Arl6 is central for cilia signalling but not essential for cilia formation (*39*, *40*). Arl13b was demonstrated to be required for ciliogenesis (*15*). Importantly, Arl6 and Arl13b were identified to cause diseases in humans when mutated, leading to Bardet-Biedl syndrome (BBS) and Joubert Syndrome (JBTS), respectively.

Arl13b is an unusual Arl protein. Whereas most members of Arl subfamily are approximately 20 kDa in mass and composed by only the guanine nucleotide-binding domain (*41–43*), this protein has a long C-terminal domain that contains a coiled-coil motif and a proline-rich region. Consequently, the molecular weight of Arl13b is approximately 48 kDa. It has been shown that the N- and C-terminal domains of Arl13b are required for its ciliary localization (*10*). Furthermore, Arl13b has also been implicated in endocytic recycling traffic (*22*), cellular differentiation (*44*) and cell migration (*23*).

Sequence analyses revealed that Arl13b contains a palmitoylation motif in its N-terminal domain that was shown to be required for membrane association, and also a SUMOylation motif that was found to regulate the targeting of different sensory receptors, and therefore downstream signalling (*17*, *45*).

Studies in *hnn* mouse mutants, carrying a null allele of *Arl13b*, show that this protein is crucial for the organization of outer-doublet microtubules of the ciliary axoneme (*15*), since the B-microtubules are neither closed nor attached to the A-microtubules. This suggests that one of the functions of Arl13b is the assembly and maintenance of the ciliary axoneme (*46*). However, the mechanism by which Arl13b regulates this function is unknown.

1.3 Ciliary trafficking

There are two processes of ciliary cargo transport. Within the axoneme, ciliary proteins are transported by intraflagelar transport (IFT), a bidirectional trafficking system that ensures the transport of ciliary cargo from the base to the tip of the cilium and backwards. The IFT machinery can be divided in two complexes, IFT-A (IFT144, IFT140, IFT139, and IFT122) and IFT-B (IFT172, IFT88, IFT81, IFT80, IFT74, IFT57, IFT52, IFT46, IFT27, and IFT20) (*47*). IFT involves movement of large protein complexes called IFT particles, or trains. Importantly, since cilia do not possess protein synthesis machinery, ciliary proteins have to be transported from intracellular compartments to cilia, using the vesicular trafficking pathways (*1*, *5*, *9*).

Ciliary targeting signals (CTS) are present in the C-terminal region of ciliary transmembranar proteins (*5*). The first CTS identified was that from rhodopsin. This protein contains a CTS of the VxP type (QVSVPA) (*1*) that is also present in polycystin 2 (PKD2). Another common CTS motif is the AQ box, present in the third intracellular loop of GPCRs that localize to the cilia, like somatostatin receptor 3 (SSTR3) and 5-hydroxytryptamine receptor 6 (5-HTR6) (*1*). Interestingly, CTS motifs have been shown to integrate lipid rafts through post-translational modifications like myristoylation, SUMOylation and/or palmitoylation (*1*, *5*, *17*). Strikingly, mutations in the CTS impair the ciliary targeting and localization of PKD2, SSTR3 and 5-HTR6 (*1*, *48*, *49*).

1.3.1 Intraflagellar transport

Kinesin-2 motors and the IFT-B complex, ensure transport within the axoneme of ciliary cargo from the base to the distal tip of the cilium in an anterograde direction, to the plus-ends of microtubules. This transport is required for cilia assembly and correct localization of ciliary receptors. Dynein-2 motors and the IFT-A complex that carry turnover product direct the transport from the tip to the base of the cilium in a retrograde direction, to the minus-end. These are then transported into the cell body for recycling or degradation. This retrograde transport is also necessary for cilia disassembly (*1*, *5*, *14*, *50*).

1.3.2 Transport from intracellular compartments to the cilium

Several models have been proposed for the routes followed by ciliary cargoes until they reach the cilium: polarized exocytosis of membrane proteins from the TGN directly to the ciliary pocket; incorporation of ciliary membrane proteins into the plasma membrane and movement into the ciliary membrane by lateral diffusion; and trafficking from the ERC to the

ciliary pocket. A schematic representation of these three models can be seen in Figure 3. It should be noted that these models are not mutually exclusive and that different ciliary cargoes could use different pathways.

The first model proposes that vesicles from the TGN are transported to the ciliary pocket at the base of the cilium, where they fuse with the ciliary membrane and then enter the cilioplasm (*1*). The IFT20 protein localizes at the ciliary pocket and the Golgi apparatus and has been shown to be necessary for the trafficking of PKD2 to the cilium. (*51*). These findings suggest that a possible function of IFT20 is the sorting of vesicles that are destined for the ciliary pocket at the TGN. The vesicles are then transported along microtubules to the base of the cilia and fuse with the ciliary membrane (*5*, *51*, *52*).

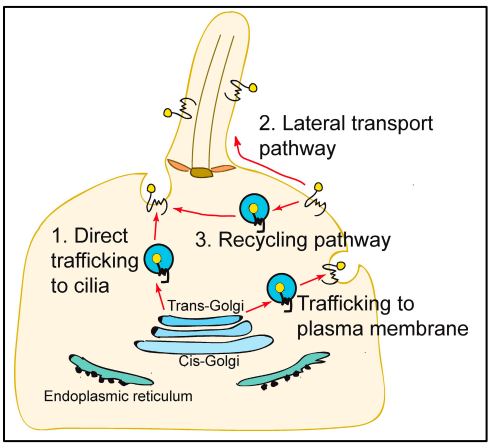

Figure 3 – Models for the trafficking of membrane proteins to cilia. (1) Direct trafficking from the Golgi to the ciliary pocket. (2) Transport to the cell surface followed by lateral transport into the cilium. (3) Internalization into the ERC (recycling pathway) and trafficking to the ciliary pocket. Taken from Milenkovit *et al*, 2009 (*53*).

The second model of ciliary membrane protein trafficking postulates a lateral transport route. Studies with Smoothened (Smo), a ciliary GPCR that after Patched receptor activation by Hedgehog is translocated to cilia, demonstrate that upon inhibition of the endocityc pathway, Smo continues to be transported to cilia by lateral diffusion. This supports the existence of lateral transport of ciliary cargoes from the plasma membrane to the cilium (*5*, *53*). However, it remains to be shown how the ciliary proteins pass the diffusion barrier between the plasma membrane and the ciliary membrane.

The third model is based on polarized exocytosis, in which the proteins are transported in vesicles from the TGN towards the ciliary pocket and then delivered to the ciliary membrane by fusion. This is illustrated by Rab11-Rabin8-Rab8 ciliogenesis cascade (*1*, *5*, *54*). Rab8 is the last GTPase in this cascade and regulates polarized vesicular traffic and carrier fusion. Rab11 is essential for Rab8 activation, since it activates Rabin8, a GEF that favors the GDP release from Rab8, converting it to its active state (*54*, *55*). When Rab8

is active, it directly interacts with ciliary cargoes like Rhodopsin, Polycystin-1 (PKD1) and Fibrocystin promoting the docking and fusion of vesicles to the ciliary membrane (*24*, *54*, *56*).

The need for vesicular trafficking pathways in cilia assembly and maintenance suggests an important role for this type of transport in cilia biology. Indeed, defects in these pathways affect the correct formation and function of this organelle, leading to several diseases collectively known as ciliopathies.

1.4 Ciliopathies

Ciliopathies are a broad and heterogeneous group of diseases that affect several organs and systems and are caused by defects in cilia. This group of diseases includes autosomal dominant polycystic kidney disease (ADPKD), Bardet-Biedl syndrome (BBS), Joubert syndrome (JBTS), Nephronophtisis (NPHP), and Meckel-Gruber syndrome (MKS), among others. More than 50 genes are known to be involved. Interestingly, different mutations in the same gene can cause different diseases with pleiotropic phenotypes and several ciliophaties are caused by mutations in different genes (*2*, *40*, *49*, *57*).

1.4.1 Joubert syndrome

Joubert syndrome (JBTS) is an autosomal recessive ciliopathy characterized by retinal dystrophy, cystic renal disease, polydactyly, hindbrain malformation, known as the 'molar tooth sign', along with ataxia and cognitive dysfunction. Furthermore, the genes affected in JBTS are all required for ciliogenesis. Consequently, mutations in these genes lead to the absence or shorter primary cilia, as well as impaired ciliary motility (*37*, *49*, *57*).

One of the genes associated with JBTS is *ARL13B.* Indeed, two missense mutations in *ARL13B* were linked to JBTS, R79Q, localized in the Arf-domain and R200C, localized in the coiled-coil motif. R79 is speculated to be critical for establishing the proper GTP-bound conformation of Arl13b that is required for effector binding. R200C mutation is thought to destabilize the position of the helix α6 of the coiled-coil region relative to the Arf-domain, suggesting that a fixed orientation of the coiled-coil region is crucial for correct Arl13b function (*43*).

Recently, a mutation in one of the exocyst complex subunits, Exo84 was found to cause JBTS in human families (*58*). The exocyst is a multi-subunit complex consisting of eight proteins, Sec3, Sec5, Sec6, Sec8, Sec10, Sec15, Exo70 and Exo84. This complex is thought to be essential for polarized exocytosis and to mediate the tethering of secretory vesicles to the plasma membrane before SNARE-mediated fusion (*18*, *59*, *60*). Interestingly,

the exocyst was found to localize to the primary cilium and to be essential for ciliogenesis (*60*). Moreover, it is a downstream effector of Rab8 and Rab11 (*54*).

Since mutations in both Arl13b and a subunit of the exocyst were found in patients with JBTS and both are involved in ciliary cargo trafficking, it is possible that an interaction between the exocyst and Arl13b occurs in ciliogenesis.

2 Hypothesis and objectives

We hypothesize that Arl13b regulates ciliary cargo trafficking from compartments of the endocytic recycling pathway to the cilium through an interaction with the exocyst complex, thereby controlling cilia biogenesis and function. Therefore, the specific aims of this work were:

Aim 1: To confirm and characterize the interaction between Arl13b and the exocyst in ciliated cell lines.

Aim 2: To assess the function of the interaction between Arl13b and the exocyst in ciliogenesis.

3 Materials and Methods

3.1 Cell Culture

All cell lines used in this worked were cultured at 37ºC with 5% CO_2. Hela and MDCK cell lines were grown in Dulbecco's Modified Eagle's Medium (DMEM, Invitrogen) supplemented with 10% heated-inactivated fetal bovine serum (FBS, Invitrogen), 100 U/ml penicillin G, 100 µg/ml streptomycin, 2mM L-glutamine and 20mM Hepes (Invitrogen). NIH-3T3 cells were grown in the same conditions but supplemented with 10% heated-inactivated bovine calf serum (BCS, Sigma). IMCD3 cells were grown in Dulbecco's Modified Eagle Medium/Nutrient Mixture F-12 (DMEM/F-12, Invitrogen) supplemented with 10% heated-inactivated FBS (GIBCO), 100 U/ml penicillin G and 100 µg/ml streptomycin (Invitrogen). To induce cilia formation, IMCD3 cells were serum-starved for 48h and NIH-3T3 cells were starved for 24h.

Cell lines were lysed in cold lysis buffer (50 mM Tris-HCl pH 7,5, 10% Igepal, 150 mM NaCl, 1 mM EDTA, 1 mM EGTA, 2 mM $MgCl_2$, 1 mM DTT), in the presence of protease and phosphatase inhibitors, for 30 minutes at 4ºC with constant agitation followed by centrifugation at 20000 *g* for 30 minutes at 4ºC. Supernatants were collected and protein concentration was determined using DC protein assay kit (Bio-Rad).

3.2 Silencing assays

Arl13b and Sec8 silencing was achived using siGENOME SMARTpool (Thermo Scientific) specific for *Mus musculus* Arl13b and Sec8. Control siRNA was done with non-targeting siRNA pool (Thermo Scientific). NIH-3T3 cells were transfected with 80 nM siRNA with Dharmafect 1 transfection reagent (Thermo Scientific) according to the manufacturer's instructions. NIH-3T3 cells were serum-starved after 48h of transfection with siRNA for 16h prior to fixation or pellets collection.

The target sequences used for Arl13b siRNA were; CUAAGACACCCGAGGAUAU, GAAUUAUUAUGCUGAAUCC, GAAACAAAGGAGACAAUGU and GGUAAUAUUUGUUGUGGAU, for Sec8 siRNA the following sequences were used; UCACUAACUCGAGGAAUAA, GGGCAAAGGAUGAUGAUAU, CGUCAUAUUCCAUCCAUUA and CAACUAAGCUAUGCCAGUA.

3.3 Plasmid transfection and constructs

The following plasmids were used: pEGFP-C-CMV5 Arl13b construct was a kind gift from Dr. K. Kontani (University of Tokyo, Japan). Arl13b 1-193-EGFP mutant and Arl13b-FLAG constructs were described previously (*22*). pGBKT7-Sec8-Myc construct was a kind gift from Dr. Joshua Lipschutz (University of Pennsylvania, United States of America). Arl13b [194-428]-EGFP was generated by removing Arl13b from the vector pEGFP-C-CMV5 Arl13b and replacing it by Arl13b [194-428] by A. Portelinha and D. Barral (unpublished).

Plasmid transfections were done using Turbofect (ThermoScientific) in HeLa and NIH-3T3 or with Lipofectamine 2000 (Invitrogen) in IMCD3 cells, according to the manufacturer's instructions.

3.4 *In vitro* protein translation

Proteins were produced using TnT® T7 coupled reticulocyte lysate system (Promega) by mixing 40 µl of TnT® T7 Quick Master Mix with 1 µl of Methionine at 1 mM, 2 µg of plasmid DNA template and nuclease-free water to a final volume of 50 µl. The mixture was incubated at 25ºC for 90 minutes to synthesize *in vitro* the proteins from the plasmid DNA template.

3.5 Immunoprecitation

For immunoprecipitation, cell lysates were pre-cleared for 1 hour with Protein G-Sepharose beads (Sigma). Samples were then incubated with GTPγS (0,5 mM, Sigma) or GDP (5 mM, Sigma) for 10 minutes at room temperature (RT). Immunoprecipitation was performed overnight at 4ºC with constant agitation, using 3 µg of anti-Arl13b (Barral et al, 2012), 2 µg of anti-Sec8 (Enzo life Science), 2 µg of anti-Myc (Calbiochem) or 2 µg of anti-FLAG (Sigma). ProteinG-Sepharose beads were then added and mixed for 4 hours at 4ºC with rotation. Beads were recovered by centrifugation at 20000 *g* for 5 minutes at 4ºC, washed once with lysis buffer with high salt concentration (500 mM NaCl), three times with lysis buffer, and finally resuspended in Laemmli sample buffer. After boiling at 94ºC for 5 minutes, the immunoprecipitates were resolved by SDS-PAGE followed by immunoblotting.

3.6 GFP-pull-down

To pull down Arl13b-EGFP, GFP-trap beads (Chromotek) were used with 800 µg of HeLa total cell lysates overexpressing the different constructs (Arl13b-EGFP, Arl13b [1-193]-

EGFP and Arl13b [194-428]-EGFP). Samples were incubated with GTPγS (0,5 mM, Sigma) or GDP (5 mM, Sigma) for 10 minutes at RT. Immunoprecipitations were performed at 4ºC for 2 hours with constant mixing. Beads were then recovered by centrifugation at 2500 *g* for 3 minutes at 4ºC, washed once with lysis buffer with high salt concentration (500 mM NaCl), three times with lysis buffer, and finally resuspended in Laemmli sample buffer. After boiling at 94ºC for 5 minutes, the immunoprecipitates were resolved by SDS-PAGE followed by immunoblotting. Alternatively, instead of directly resuspended the beads, they were eluted with 0,2 M glycine pH 2,5 for 30 seconds under constant mixing at RT, followed by centrifugation, and then neutralized with 1 M Tris HCl pH 10.4. This step was repeated twice to increase the elution efficiency. After elution, samples were dialysed in lysis buffer without protease and phosphatase inhibitors, under constant mixing at 4ºC overnight with Snakeskin dialysis membrane with a cut-off of 10 kDa molecular weight (Thermo Scientific). The buffer was replaced once and dialysis proceeded in the same conditions for 4 hours. Dialyzed samples were then resolved by SDS-PAGE followed by immunoblotting.

3.7 Immunobloting

Samples were resolved by SDS-PAGE and transferred onto nitrocellulose membranes in transfer buffer (25 mM Tris; 192 mM glycine; 0,5% SDS; 20% Methanol) for 90 minutes at 500 mA and processed for immunoblotting. Membranes were blocked with blocking buffer (5% skimmed milk and PBS with 0.1% Tween-20) and the antibodies incubated in the blocking buffer. Anti-Arl13b (Barral et al*.,* 2012) was used at 0.6 μg/ml, anti-GAPDH (Glyceraldehyde-3-phosphate dehydrogenase, SicGen) at 0.2 μg/ml, anti-Sec8 (Enzo life Science) at 0.2 μg/ml, anti-GFP (Sicgen) at 0.2 μg/ml, anti-FLAG (Sigma) at 0.7 μg/ml, anti-Myc (Calbiochem) at 0.1 μg/ml, anti-Exo70 (Milipore) at 0.1 μg/ml and HRP-conjugated secondary antibodies (GE Healthcare) were used at 0.7 μg/ml. Blots were developed with Clarity™ Western ECL substrate (Bio-Rad) or Amersham ECL Prime (GE Healthcare) according to the manufacturer's instructions and a Molecular Imager Chemidoc XRS (Bio-Rad) was used to detect the chemiluminescence. Band intensities were quantified using *ImageJ* software and normalized using GAPDH or GFP.

3.8 Immunofluorescence

Cells grown on glass coverslips were serum-starved for 24 (NIH-3T3) or 48 hours (IMCD3), washed with PBS and fixed in 4% paraformaldehyde in PBS for 15-20 minutes at RT. Then coverslips were permeabilized and block with PBS, 0.5% BSA and 0.1% saponin for 15 minutes at RT. Next slices were incubated for 1 hour at RT with primary antibody such

as anti-Arl13b antibody (kind gift from Tamara Caspary, Emory University, USA) and anti-acetylated tubulin (Sigma). The slides were then washed five times with PBS, 0.5% BSA and 0.1% saponin. Secondary Alexa fluor 488- or 568-conjugated anti-rabbit or anti-mouse antibodies (Invitrogen) were incubated in the PBS, 0.5% BSA and 0.1% saponin for 1 hour at RT and washed once and the nuclei were stained with DAPI in the same buffer for 10 minutes at RT. After washing three more times coverslips were mounted in mounting medium (15% w/v vinol 205, 33% v/v glycerol, PBS in 0.1% azide) and analyzed in a Zeiss LSM 710 confocal microscope equipped with a Plan-Apochromat 63/1.40 Oil Ph3 lens and Zeiss Zen 2010 software. Images were processed with *ImageJ* software adjusting the levels or brightness of each channel up to a maximum threshold defined by the absence of signal in the negative controls stained with irrelevant IgG antibodies.

3.9 RNA extraction, complementary DNA production and real-time quantitative PCR

RNA from cells lysates was extracted with RNeasy Mini Kit (Qiagen) according to the manufacturer's instructions. One µg of total RNA was reverse-transcribed to synthesize complementary DNA (cDNA). Samples were incubated with 10 mM dNTPs mix (Thermo Scientific) and random primers (Sigma) at 65ºC for 5 minutes. Samples were then incubated with 5x buffer (Invitrogen), DTT (Invitrogen) and RNAseOUT (Invitrogen) at 25ºC for 5 minutes, and finally incubated with Superscript II (Invitrogen) first at 25ºC for 10 minutes, then at 42ºC for 50 minutes and finally at 70ºC for 15 minutes. For the real-time quantitative PCR (qRT-PCR), Brilliant SYBR® Green QPCR Master Mix (Roche) was used according to the manufacturer's instructions and the analysis was done in a qPCR Roche Lyghtcycler (Roche).

The primers used were 5'-GAATCCAAGGAGAATACCCTG-3' (forward) and 5'-CCAACACCAATATAGGCTTTCC-3' (reverse), for Arl13b, 5'-GGAAATACAGGAGCACAGTCAG-3' (forward) and 5'-CACGGTCACACTTCTCATAGG-3' (reverse), for Sec8, 5'-CATTTCCTGGTATGACAACGA-3' (forward) and 5'-GTCTACATGGCAACTGTGAG-3' (reverse), for GAPDH used to normalize the values of expression.

4 Results

Cecília Seixas performed Figure 4A, 4C and Supplementary Figure 1 and I performed all the remaining work with her assistance.

4.1 Characterization of the interaction between Arl13b and the exocyst complex

Several small G proteins belonging to the Rho, Rab, and Arf families interact with exocyst subunits to regulate the function of this complex (*61–64*). Moreover, mutations in the exocyst subunits or Arl13b cause Joubert syndrome in human families (*58*), suggesting a link between the exocyst and Arl13b. Since Sec8 is present in cilia (*60*, *65–67*), we investigated the existence of an interaction between the exocyst complex and Arl13b through Sec8 subunit.

4.1.1 Sec8 is an Arl13b effector

We tested if there is an interaction between Arl13b and Sec8, by immunoprecipitations. A specific Arl13b antibody was used to capture Arl13b from total lysates of mouse inner medullary collecting duct (IMCD3) cells and, immunoprecipitates were probed for the presence of Sec8 by immunoblot (Fig. 4).

Since small G proteins preferentially bind effectors in their GTP-bound, active state, we incubated cell lysates with GTPγS, a non-hydrolyzable form of GTP, or GDP, as a control, prior to performing the immunoprecipitations, as described in Materials and Methods. We found that the pre-incubation with GTPγS dramatically increases the co-immunoprecipitation of Sec8 with Arl13b when compared to the pre-incubation with GDP (Fig. 4A). We regularly observed lower levels of non-specific Sec8 binding to the beads (e.g., see Fig. 4A, IgG lane). Moreover, we used the reverse strategy, *i.e.* we immunoprecipitated Sec8 from total cell lysates of ciliated IMCD3 cells and probed for Arl13b by immunoblotting (Fig. 4D). We observed again a GTP-dependence for the interaction between Arl13b and Sec8. These data are consistent with our hypothesis of Sec8 exocyst subunit serving as an effector of Arl13b.

To show that this interaction was not restricted to IMCD3 cell line, we also tested ciliated mouse embryonic fibroblasts (NIH-3T3) and Madin-Darby canine kidney (MDCK) cells. The results confirmed that Sec8 preferentially co-immunoprecipitates with active Arl13b independent of the cell line used (Fig.4B and C). Furthermore, we also immunoprecipitated Arl13b from non-ciliated HeLa cells and found that Sec8 also interacts with Arl13b in this cell line, showing that this interaction is conserved and not dependent upon the presence of cilia (Supplementary Fig. 1).

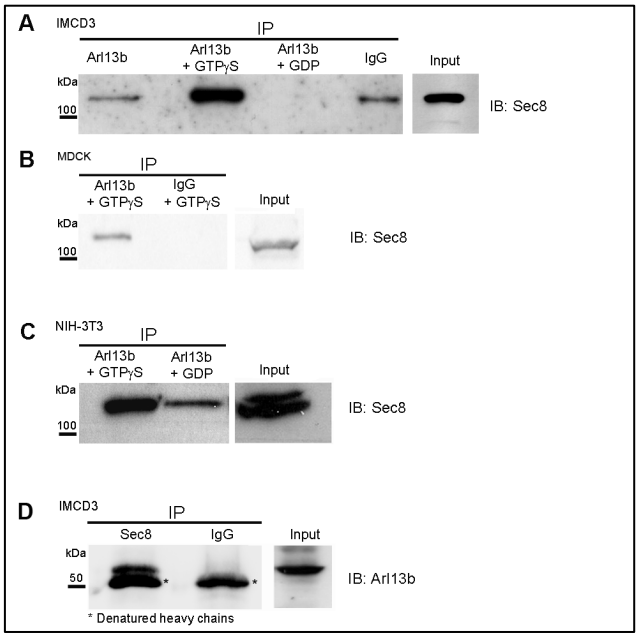

Figure 4 – Sec8 and Arl13b co-immunoprecipitation in total cell lysates of ciliated and non-ciliated cells. Total cell extracts were prepared and used for co-immunoprecipitation. Immunoprecipitates were resolved by SDS-PAGE. **(A)** IMCD3 cells (600 μg protein) after pre-incubating with no nucleotide (left lane), GTPγS (0,5 mM; 2nd lane), GDP (5 mM, 3rd lane) or a non-specific rabbit IgG, as control (4th lane), samples were immunoprecipitated with Arl13 follow by immunoblotting with anti-Sec8 antibody. **(B)** MDCK cells prepared as described in (A). **(C)** NIH-3T3 cells prepared as described in (A). **(D)** IMCD3 cells (600 μg protein) immunoprecipitated with Sec8 or a non-specific IgG, as control, follow by immunoblotting with anti-Arl13b antibody. Asterisks (*) indicate the denatured heavy chains, absent in the cell lysate (input).

4.1.2 Sec8 and Arl13b interact directly

Since Sec8 belongs to a multi-subunit complex, the exocyst, we asked if Arl13b interacts directly with this subunit. For that, Sec8-Myc and Arl13b-FLAG were separately translated *in vitro* by a transcription and translation (TNT) T7 polymerase-coupled reticulocyte lysate system using plasmids encoding the C-terminal tagged proteins as templates. The reliability of this system to generate the tagged proteins *in vitro* was confirmed by immunoblotting (Fig. 5A). The synthesized proteins were then mixed and incubated in the presence of GTPγS. Immunoprecipitation was performed with anti-FLAG monoclonal antibody and the immunoprecipitated products were analyzed by immunoblot with anti-Myc antibody. We observed that the *in vitro*-translated Sec8-Myc co-precipitates with Arl13b-FLAG, suggesting that these two proteins interact directly (Fig. 5B, lane 1, asterisk). As an internal control, we performed the immunoprecipitation with an irrelevant IgG. In this case, we detected a faint band by immunoblotting with anti-Myc antibody that corresponds to the Sec8-Myc that bound to the beads non-specifically (Fig. 5B, lane 2). This band is noticeably fainter than the one co-immunoprecipitated with Arl13b-FLAG and

represents non-specific stickiness of Sec8 to the beads, as described. Additionally, we performed an immunoprecipitation with anti-FLAG antibody using as input a mixture of *in vitro*-translated Arl13b-FLAG with a TNT reaction in which no DNA was added as template. As expected, we failed to detect a band by immunoblotting with the anti-Myc antibody (Fig. 5B, lane 3).

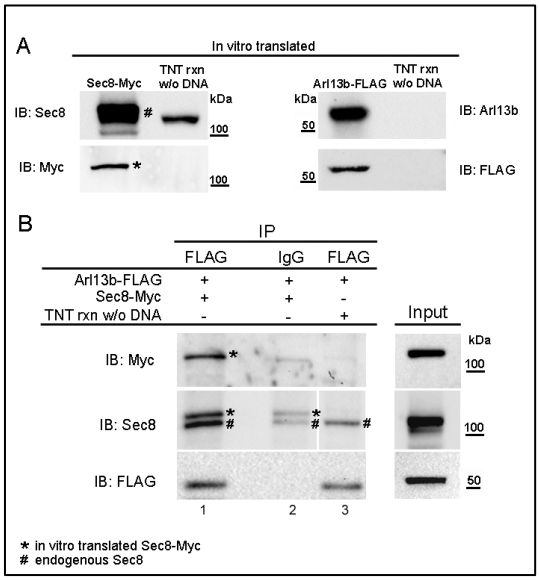

Figure 5 – Sec8 and Arl13b interact directly. (A) Sec8-Myc and Arl13b-FLAG were *in vitro*-translated using the transcription and translation (TNT) T7 coupled reticulocyte lysate system. Five percent of the input was resolved by SDS-PAGE and analyzed by immunoblotting with anti-Sec8, anti-Myc, anti-Arl13b or anti-FLAG antibodies. As a control, a TNT reaction without DNA as template was analyzed to distinguish the endogenous levels of the proteins in the reticulocyte lysates from the *in vitro*-translated proteins. **(B)** Immunoprecipitation with anti-FLAG antibody was performed using as input a mixture of the *in vitro*-translated proteins, in the presence of GTPγS. Immunoprecipitates (lane 1) were analyzed by immunoblot with anti-Myc, anti-Sec8 or anti-FLAG antibodies. As a negative control, immunoprecipitations were performed with an irrelevant mouse IgG_1 (IgG) (lane 2), or with an anti-FLAG antibody using as input a TNT reaction with no DNA as template that was mixed, in the presence of GTPγS, with *in vitro*-translated Arl13b-FLAG (lane 3). Asterisks (*) indicate *in vitro*-translated Sec8-Myc and the pound (#) signs indicate endogenous Sec8.

Thus, our data clearly demonstrates that Sec8 does not need to be present in the exocyst complex in order to be co-immunoprecipitated with Arl13b, and supports a direct interaction between Arl13b and Sec8.

4.1.3 Exo70 co-immunoprecipitates with Arl13b

Since we have demonstrated that Sec8 directly binds to Arl13b, we wondered if other subunits of the exocyst were also co-immunprecipitated with Arl13b in ciliated cell lines. To assess this, we performed an immunoprecipitation assay in MDCK and NIH-3T3 cells. For this, total MDCK cell lysate was pre-incubated with GTPγS and then incubated with anti-

Arl13b antibody, or an irrelevant IgG as a negative control. The immunoprecipitates were then analyzed by immunoblot using anti-Exo70 antibody (Figure 6A). We observed a band with the expected molecular weight for Exo70 in the lane where the product of immunoprecipitation with Arl13b was separated, suggesting that Exo70 co-immunoprecipitates with Arl13b. We also tested the interaction between Arl13b and Exo70 in NIH-3T3 cells (Figure 6B). For this, total NIH-3T3 cell lysates were pre-incubated with GTPγS or GDP and then incubated with anti-Arl13b antibody. The immunoprecipitates were then analyzed by immunoblot using anti-Exo70 antibody. In this case we obtain a similar results since Exo70 is co-immunoprecipitated with Arl13b also in this cell line. Moreover, we found that the pre-incubation step with GTPγS dramatically increases the co-immunoprecipitation of Exo70 with Arl13b when compared to the pre-incubated with GDP. Hence, this result suggests that Arl13b interacts with the whole exocyst complex.

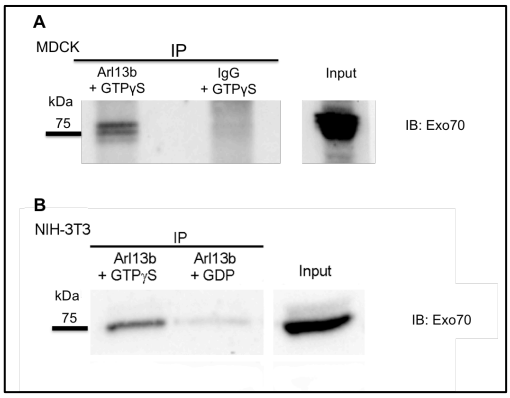

Figure 6 – Exo70 co-Immunoprecipitates with Arl13b in MDCK and NIH-3T3 cells. (A) Total cell lysates from MDCK cells (800 µg protein) were immunoprecipitated with anti-Arl13b antibody after pre-incubation with GTPγS (0,5 mM; left lane), or with a non-specific rabbit IgG as a control, also pre-incubated with GTPγS (0,5 mM; right lane). **(B)** Total cell lysates from NIH-3T3 cells (800 µg protein) were immunoprecipitated with anti-Arl13b antibody after pre-incubation with GTPγS (0,5 mM; left lane), or GDP (5 mM; right lane). Immunoprecipitates were resolved by SDS-PAGE followed by immunoblotting with anti-Exo70 antibody for both (A) and (B).

4.1.4 Sec8 and Arl13b interaction is abolished by Arl13b N- or C-terminal domain truncation

In order to characterize Arl13b-Sec8 interaction, we investigated the Arl13b domains responsible for this interaction testing by immunoprecipitation with the same system used previously which Arl13b domain interacts with Sec8. With this goal in mind, we overexpressed three forms of Arl13b tagged with GFP: a full-length Arl13b form, and two truncation mutants, Arl13b [1-193] and Arl13b [194-428]. The mutant Arl13b [1-193] contains only the Arf domain of the protein and the mutant Arl13b [194-428] contains the coiled-coil domain and the proline-rich regions (Supplementary Figure 2).

After overexpressing the different forms of Arl13b we confirmed the transfection efficiency by fluorescence microscopy. The percentage of transfection was similar for all Arl13b constructs. We analysed total cell lysate from the transfected cells by SDS-PAGE followed by immunoblot with anti-GFP antibody. The intensity of the bands corresponding to the different forms of tagged Arl13b were different, suggesting that the levels of expression of the different Arl13b forms were distinct, despite the percentage of transfection being similar (Fig. 7A). Therefore, to ensure that the same amount of each Arl13b construct was used in the immunoprecipitation, the levels of GFP-tagged Arl13b were first normalized to GAPDH and then relative to each other. However, to use similar amounts of the different Arl13b mutant proteins, the volume of cell lysate had to be different between samples, which implied also a different amount of binding partners.

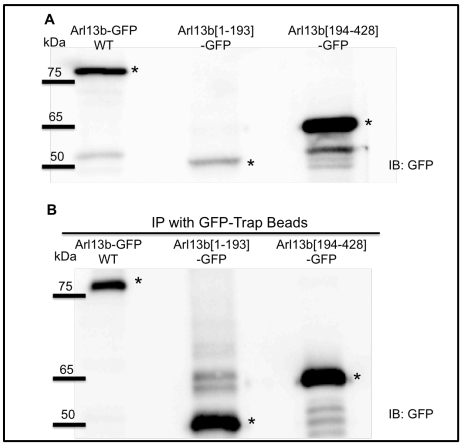

Figure 7 – Arl13b-GFP pull-downs. (A) Cell lysates from HeLa cells (80 µg protein) overexpressing Arl13b-GFP full length, Arl13b[1-193]-GFP or Arl13b[194-428]-GFP were resolved by SDS-PAGE and immunoblotted with anti-GFP antibody. **(B)** Cell lysates from HeLa cells (800 µg protein) overexpressing Arl13b-GFP full length, Arl13b[1-193]-GFP or Arl13b[194-428]-GFP were immunoprecipitated with GFP-trap beads to pull-down Arl13b proteins tagged with GFP. Asterisks (*) indicate the band for each construct.

To overcome this problem, we performed a pull-down of GFP-tagged proteins using GFP-trap beads instead of ProteinG-beads used previously. This allows the immunoprecipitation of GFP-tagged proteins as well as their binding partners. Since the beads can be saturated with Arl13b-GFP, it also allows the normalization of the levels of GFP-Arl13b mutants and binding partners. Importantly, we observed that the immunoprecipitation with the GFP-trap beads pulled-down similar levels of the three constructs (Supplementary Figure 3). We incubated total HeLa cell lysates overexpressing each construct with the GFP-trap beads in the presence of GTPγS, GDP, or no nucleotide. As a negative control, we used HeLa cell lysates overexpressing a construct encoding GFP in the presence of GTPγS. The immunoprecipitated products were analyzed by immunoblot

with Sec8 or Exo70 antibody. The results show that Sec8 and Exo70 are co-immunoprecipitated in the presence of the full-length Arl13b and GTPγS (Fig. 8A). As expected, in the presence of GDP, both Sec8 and Exo70 are immunoprecipitated at a lower level when compared with the samples incubated with GTPγS. The intensity of the band for Sec8 and Exo70 detected in the immunoblots was then normalized to the GFP band intensity for each Arl13b form. Regarding the mutants, both show impaired binding to Sec8 and Exo70 in the presence of GTPγS (Fig. 8B and 8C). This result suggests that both domains of Arl13b are required for the interaction with Sec8 and Exo70. We also observed an interaction above the background level with Sec8 and Exo70 with the mutant Arl13b [1-193]. However, it cannot be considered a biologically relevant interaction since it is significantly lower than the interaction observed with the full length Arl13b in the presence of GDP. Thus, from this experiment we can only conclude that none of the truncated Arl13b mutants can interact with Sec8 or Exo70, since the intensity of the corresponding bands is similar to the negative control done with cell lysates overexpressing GFP.

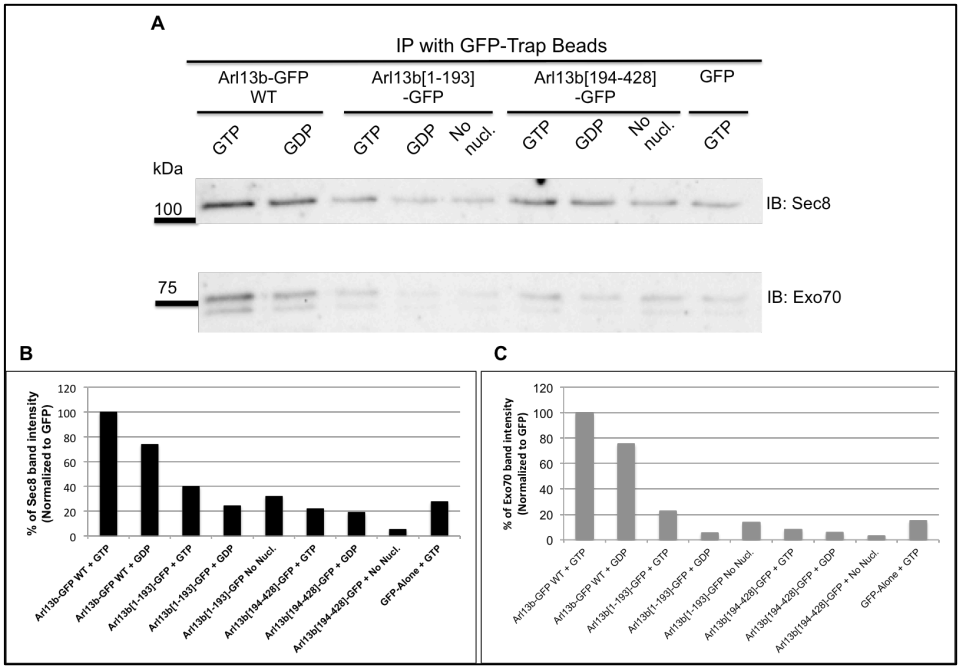

Figure 8 – Characterization of Sec8 interaction with Arl13b truncation mutants in the presence of GTPγS, GDP or no nucleotide. (A) Total lysates from HeLa cells overexpressing Arl13b-GFP full-length, Arl13b[1-193]-GFP or Arl13b[194-428] were immunoprecipitated from total cell lysates (800 µg protein) with GFP-trap beads, after pre-incubation with GTPγS (0,5 mM), GDP (5 mM) or no nucleotide. As a negative control we used total cell lysates from HeLa cells overexpressing GFP pre-incubated with GTPγS (0,5 mM) to set the background level of unspecific binding of Sec8 to the beads. Immunoprecipitates were resolved by SDS-PAGE, followed by immunoblotting with anti-Sec8 and anti-Exo70 antibodies. **(B)** Quantification of the bands intensities for Sec8 shown in (A), using ImageJ software and normalized for GFP levels. **(C)** Quantification of the bands intensities for Exo70 shown in (A), using ImageJ software and normalized for GFP levels.

4.2 Function of Arl13b-exocyst complex in ciliogenesis

Defects in ciliogenesis have been implicated in several cilopathies. Arl13b is a ciliary protein known to be involved in cilia formation/maintenance and signalling and is recognized as a central protein in ciliogenesis (*15*, *46*). Besides that, the exocyst, namely the Sec10 subunit, has been demonstrated to also play a crucial role in ciliogenesis (*18*, *59*). Therefore, since Arl13b and the exocyst are known to be ciliogenesis regulators and we found that both interact through the Sec8 subunit, we assessed if Sec8 silencing could mimic the phenotypes obtained when silencing Arl13b. If that was the case, it would further suggest that Arl13b and exocyst work in the same pathway in ciliogenesis.

4.2.1 Arl13b and Sec8 depletion affect cilia formation and length in NIH-3T3 cells

To assess if Arl13b or Sec8 depletion cause defects in cilia formation, we silenced Arl13b or Sec8 using (Small interfering RNA) siRNA pools in NIH-3T3 cells and measured the silencing levels by qRT-PCR. Silencing of 75% and 76% were obtained for Arl13b and Sec8, respectively (Supplementary Figure 4). We then measured the length of cilia in cells treated with siControl, siArl13b or siSec8 (Figure 9).

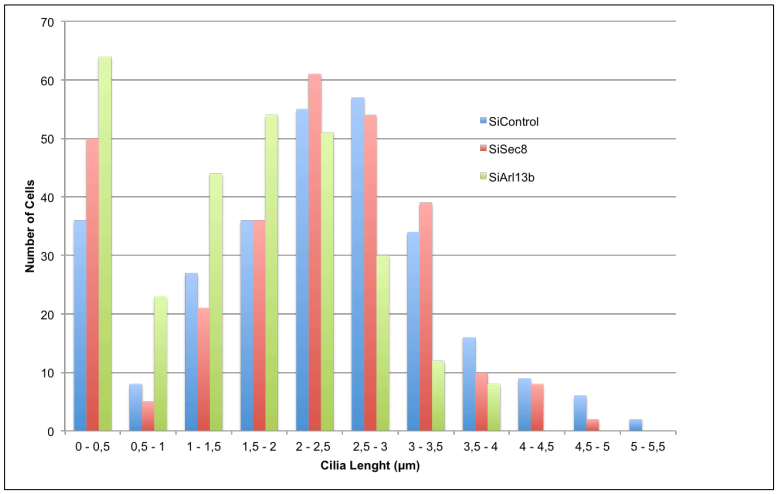

Figure 9 – Defects in ciliogenesis upon depletion of Arl13b and Sec8. Normalized histogram showing the cilia length measured in NIH-3T3 cells transfected with siRNA pools to silence Sec8 and Arl13b. A pool of siRNA control was used as control.

In cells treated with siControl, the average cilia length was 2,5 µm and they fail to grow cilia longer then 5,5 µm, while in cells treated with siArl13b the average length was 1,5 µm and cells fail to grow cilia longer than 4 µm. This reduction in cilia length and delay in

ciliogenesis was expected since Arl13b is known to be required for cilia biogenesis and maintenance (*15*, *46*). The cells treated with siSec8 showed an average cilia length of 2 μm. Furthermore, an abrogation in ciliogenesis could be perceived in these cells since they fail to grow cilia longer than 5 μm and at the same time display more cilia shorter than 0,5 μm than cells treated with siControl suggesting that Sec8 is required for proper ciliogenesis.

This result suggests that Arl13b and exocyst are in the same pathway since silencing of Arl13b and Sec8 cause similar defects in ciliogenesis. However the defects caused in absence of Arl13b are stronger than the ones observed when silencing Sec8, indicating that the cell could have a compensatory mechanism to assist in ciliogenesis in the absence of the exocyst but not in the absence of Arl13b.

5 Discussion and future perspectives

Mutations in Arl13b and the exocyst subunity Exo84 have been found in human patients with Joubert syndrome (JBTS) (*49*, *58*). Arl13b was described as a ciliary protein whose depletion leads to defects in cilia structure and function (*15*, *42*, *46*). The exocyst is a hetero-octomeric complex best known for its function in tethering exocytic vesicles to the plasma membrane. Moreover, it has recently been associated with ciliogenesis and in vesicle trafficking to the apical membrane (*59*, *60*).

Regarding our first aim, we show for the first time that Sec8 is a *bona fide* effector of Arl13b, since Arl13b co-immunoprecipitation with Sec8 is considerably increased in the presence of GTPγS. We also show that this interaction is present in different cell types and that it is not dependent upon the presence of cilia. Moreover, we found that this interaction is direct and independent of the presence of the other exocyst subunits since *in vitro*-translated Sec8-Myc co-immunoprecipitates with Arl13b-FLAG. Furthermore, this result suggests that Sec8 does not need to be present in the exocyst complex to interact with Arl13b.

Importantly, we found that both the N- and C-terminal domains of Arl13b are necessary for the interaction with Sec8. In order to characterize the interaction between Arl13b and Sec8 and to know the Arl13b domains responsible for the interaction, we performed an immunoprecipitation with GFP-trap beads, which allows the concentration of the GFP-tagged proteins expressed from the constructs of three different forms of Arl13b. Using this method, we confirmed that Sec8 is an Arl13b effector and that the binding to Sec8 requires both the N- and C- terminal domains of Arl13b. A possible explanation for the lack of the interaction in the mutant Arl13b [1-193] is that the C-terminal domain of Arl13b has an important role in the stabilization of the protein to allow the molecular conversion of GTP into GDP in the Arf domain, controlling the binding of effectors to the protein (*43*). Thus, the lack of the C-terminal domain of Arl13b would impair the GTP binding to the Arf domain and consequently the exchange from the inactive to the active state. The mutant Arl13b [194-428] does not have the Arf domain, so it has no manner of binding to GTP and exchange to the active state. Since Arl13b binds to the effector Sec8 when in the active state and this mutant fail to exchange states it was expected that the interaction fail to occur. To investigate the exact domain of Arl13b required for the interaction, new mutants need to be generated with shorter truncations and point mutations, so the protein conformation and stability is not dramatically affected and we can narrow down the amino acids necessary for the interaction to occur.

Furthermore, Exo70 is also co-immunoprecipitated with Arl13b, suggesting that Arl13b could interact with the whole exocyst complex. Since only the exocyst subunits Sec10

and Sec15 have free pools in the cell, forming a subcomplex in addition to their incorporation into the exocyst complex (*68*), it can be speculated that the interaction of Arl13b with Sec8 mediates the interaction with the whole complex. We also showed that Exo70 co-immunoprecipitates with Arl13b, both in ciliated and non-ciliated cell lines. This result supports the hypothesis that Sec8 mediates the interaction between Arl13b and the rest of the exocyst complex. Thus, to demonstrate that Arl13b-Sec8 interaction occurs in the presence of the whole exocyst complex, it will be important to investigate if the other exocyst complex subunits co-immunoprecipitate with Arl13b.

Interestingly, the transport, sorting and fusion of vesicles that transport polycystin-1 (PKD1) to cilia, requires the participation of more than one subunit of the BBSome complex, a complex comprise by seven proteins BBS1, BBS2, BBS4, BBS5, BBS7, BBS8 and BBS9 involved in intracellular trafficking (*69*) and mutated in Bardet-biedl syndrome (BBS). While BBS3/Arl6 is responsible for the ciliary trafficking of PKD1 to the ciliary base, BBS1 is responsible for the entry of PKD1 in cilia. This is also the case of α-amino-3-hydroxy-5-methyl-4-isoxazolepropionic acid (AMPA) receptors (*70*), in which Sec8 sorts and transports the AMPA receptor to neuronal axon and Exo70 assists in the fusion of the vesicles carrying AMPA receptors with the target membrane. Therefore, a similar model of action can be hypothesized for Arl13b-containing vesicles, where these vesicles follow a two-step process to enter cilia: first they are targeted to the periciliary region and then transported into the cilia in an exocyst-dependent manner. To test this hypothesis, it will be necessary to co-localize Arl13b, Sec8 and Exo70 and assess how depletion of Sec8 and/or Exo70 affects the trafficking of Arl13b to cilia. If Exo70 is responsible for the fusion of Arl13b-containing vesicles to the plasma membrane, when Exo70 is depleted, an accumulation of Arl13b-containing vesicles in the periciliary region is expected. Moreover, Arl13b will fail to enter cilia. On the other hand, when Sec8 is silenced, an accumulation of Arl13b-containing vesicles will be expected in intracellular compartments such as the endocytic recycling compartment (ERC) since our group found that Arl13b regulates endocytic recycling traffic (*22*). Of note, several studies suggest that the ERC can serve as a donor compartment for ciliary cargo (*1*, *24*). But a direct link between the role of Arl13b in endocytic recycling and its function in ciliogenesis has not yet been established. Therefore, it can be speculated that the traffic of ciliary cargo to the periciliary region is dependent on the exocyst-Arl13b complex and follows the endocytic recycling pathway through the ERC. To assess if there is a direct link between Arl13b and the endocytic recycling pathway in ciliogenesis, immunofluorescence studies with specific markers should be performed. For this, IMCD3 cells can be stained with anti-acetylated tubulin to mark cilia, anti-Rab11 antibody to label the ERC and anti-EEA-1 antibody to mark early endosomes. If Arl13b and Sec8 co-localize with these markers, it will be possible to show which intracellular trafficking pathway Arl13b-

containing vesicles are following and if the interaction between Arl13b and exocyst occurs just in the periciliary region or in an intracellular compartment to sort the vesicles to the ciliary pocket.

Therefore, in our second aim using siRNA for silencing, we observed that Sec8 and Arl13b are both necessary for cilia formation. When we silence Arl13b in NIH-3T3 cells, we observe a reduction in cilia length, being the cells unable to grow cilia longer than 4 μm and an average length of 1,5 μm while in the cells treated with siControl the cilia grow until 5,5 μm and the average length is 3 μm. This results was expected since Arl13b is known to have a role in ciliary formation and maintenance (*15*). Interestingly, we also observed an abrogation in ciliogenesis in cells silenced for Sec8. In this case, the cells fail to grow cilia longer than 5 μm and the average length is 2 μm. Importantly, we observed that there is an increase in the number of cilia that are shorter than 0,5 μm in cells silenced for Sec8 and Arl13b, suggesting that some cells cannot extend their axoneme when depleted for both Arl13b and Sec8. In contrast, others report that Sec8 silencing does not affect cilia formation (*59*). But those authors did not rule out the possibility that the lack of a phenotype was due to insufficient silencing of the protein. More studies need to be done to fully understand how Sec8 depletion affects ciliogenesis. It will also be necessary to look at the intracellular localization of Arl13b when cells are depleted to Sec8 and the other way around, to know if the proteins are failing to enter the cilia and if that is one possible explanation for the observation of shorter cilia observed by us in cells depleted for Sec8. Since exocyst is required for ciliogenesis and given the importance of Arl13b for formation and function, our findings could be extended to which ciliary proteins depend on Arl13b-exocyst regulation to reach the cilia, to allow understanding the etiology of JBTS. For this, it should be done assays in live cells expressing ciliary cargos regulated by Arl13b or by exocyst such as fluorescence recovery after photobleaching (FRAP) assays. This technique, as the name suggests, consists in photobleaching the fluorescent protein with a laser until the fluorescence is partially or completely lost. Then, the time of fluorescence recovery is monitored, giving information about the time that the protein takes to be transported from intracellular compartments and whether it is being imported to or exported from cilia (*46*, *71*). To perform this study, a ciliated cell line that stably expresses 5-HTR6 fused to GFP (IMCD3-HTR6-GFP) can be used. Notably, it has been shown that Arl13b depletion results in defective dynamics of 5-HTR6 within cilia (*44*). Therefore, it is expect to observe defects in the ciliary transport of 5-HTR6 from cytosol to cilia when Arl13b is depleted. If Sec8 assists in the transport of Arl13b-containing vesicles to cilia, it is expect to observe a similar phenotype when Sec8 is depleted. Thus, these experiments will determine if Arl13b and/or the exocyst regulate ciliary cargo trafficking through the same route.

We intended to investigate if there was a synergistic genetic interaction between Arl13b and the exocyst and to study the functional relevance of their interaction using zebrafish as an animal model. We planned to silence the proteins through morpholinos (MO) injection in one stage-cell embryos of zebrafish. MOs are small antisense oligos specific for small RNA regions preventing the expression of a protein of interest. Nevertheless, we were interested in the effects of this synergistic interaction between Arl13b and the exocyst in the formation of the Kupffer's vesicle (KV), the fish homologue of the mouse node. The KV is responsible for generating a directional fluid flow derived by motile cilia that leads to the left-right asymmetry of the internal organs during development (*72*). Therefore, we wanted to assess how cilia formation in the KV is affected between the stages of 8 and 12 somites, period in the fish development when the KV starts to form and the cells start to ciliate. To investigate if there is a synergy between the two genes, the embryos are submitted to a sub-optimal dose of both MOs for Arl13b and exocyst simultaneously, in which the embryos do not present any phenotype, when compared to control-injected embryos. We planned to measure the cilia length in the KV of the double morphants and to correlate shorter cilia with left-right patterning defects eventually detected.

It is known that Sec8 knockout mice display early embryonic lethality (*73*). Depletion of Sec8 in zebrafish embryos could also cause early development defects that would preclude the analysis of specific phenotypes (*60*). Therefore, we decided to use a MO for Sec10, since this subunit is known to be the core of the exocyst complex and this silencing was alredy successfully acomplished in zebrafish (*59*). Thus, to investigate the synergistic effects of double morphant Arl13b-Sec10 in the KV cilia, we started by optimizing the dose of each MO in order to reach a sub-optimal dose that does not cause any noticeable phenotype. This optimization was done by injecting 3 different doses of MO for Arl13b in one stage-cell embryos and by looking at 3 different parameters; death rate, body curvature and left-right asymmetry of the heart. The sub-optimal dose was achieved when the percentage of dead embryos was lower than 50%, no body curvature phenotype was seen and there was at least 90% of left-sided heart morphants (*42*). The sub-optimal dose for Arl13b was achieved injecting 0,15 mM of MO in zebrafish embryos. Unfortunately, the sub-optimal dose for Sec10 MO has not yet been determined due to limitation of time. Therefore, this aim will have to be continued.

Our collaborator Dr. Josh Lipschutz, an expert in exocyst, performed a similar experiment in the meantime but focusing only their observations in cilia-related phenotypes like curved tail, small eyes and pericardial edema. Although they have not analysed KV and other ciliated organs that we intend to look at, their experiment showed that there is a synergistic genetic interaction between Arl13b-Sec10 for cilia-related events. This result indicates that these genes act in a common or parallel pathways.

In conclusion, our study reveals a novel effector of Arl13b, the exocyst. We showed that the interaction between exocyst and Arl13b is mediated by a direct interaction with Sec8. Besides we also proved that both the N- and C- terminal domain of Arl13b are necessary for the interaction with Sec8. Moreover, we showed that Exo70 is co-immunoprecipitated with Arl13b. We observed for the first time, that Sec8 causes ciliogenesis abrogation in mammalian cell line. Taking into account these results, and the results from our collaborator that there is a synergistic genetic interaction between Arl13b and Sec10, and considering that Arl13b regulates endocytic recycling trafficking through the ERC (*22*), we propose a model where Arl13b and the exocyst are involved in the transport of ciliary cargo derived from the ERC. In our model, Sec8 is responsible for sorting and transport of Arl13b-containing vesicles to the periciliary region. Exo70 could be requiredfor the fusion of these vesicles to the ciliary pocket membrane, since Exo70 is a membrane-bound protein known to be involved in plasma membrane remodelling and actin dynamics (*74*). A similar role was proposed for Rab10, which localizes at the base of nascent cilia with exocyst subunits, and forms a complex with Sec8 (*66*). Future studies will explore if this model is correct and should bring more insights in the role of Arl13b in ciliogenesis.

6 References

1. M. V Nachury, E. S. Seeley, H. Jin, Trafficking to the ciliary membrane: how to get across the periciliary diffusion barrier? *Annu. Rev. Cell Dev. Biol.* **26**, 59–87 (2010).

2. P. Satir, L. B. Pedersen, S. T. Christensen, The primary cilium at a glance. *J. Cell Sci.* **123**, 499–503 (2010).

3. Y.-N. Ke, W.-X. Yang, Primary cilium: an elaborate structure that blocks cell division? *Gene*. **547**, 175–185 (2014).

4. J. T. M. L. Paridaen, M. Wilsch-Bräuninger, W. B. Huttner, Asymmetric inheritance of centrosome-associated primary cilium membrane directs ciliogenesis after cell division. *Cell*. **155**, 333–44 (2013).

5. J. Malicki, T. Avidor-Reiss, From the cytoplasm into the cilium: bon voyage. *Organogenesis*. **10**, 138–57 (2014).

6. Vieira, Otilia V; Gaus, Katharina; Verkade, Paul; Fullekrug, Joachim; Vaz, Winchil L C; Simons, Kai, FAPP2, cilium formation, and compartmentalization of the apical membrane in polarized Madin-Darby canine kidney (MDCK) cells. *Proc. Natl. Acad. Sci. U. S. A.* **103**, 18556–61 (2006).

7. C. Hoerner, T. Stearns, Remembrance of cilia past. *Cell*. **155**, 271–3 (2013).

8. S. Takeda, K. Narita, Structure and function of vertebrate cilia, towards a new taxonomy. *Differentiation.* **83**, S4–11 (2012).

9. A. M. Fry, M. J. Leaper, R. Bayliss, Guardian of organ development and homeostasis. **10**, 62–68 (2014).

10. Y. Hori, T. Kobayashi, Y. Kikko, K. Kontani, T. Katada, Domain architecture of the atypical Arf-family GTPase Arl13b involved in cilia formation. *Biochem. Biophys. Res. Commun.* **373**, 119–24 (2008).

11. Garcia-Gonzalo, Francesc R; Corbit, Kevin C; Sirerol-Piquer, María Salomé; Ramaswami, Gokul; Otto, Edgar A; Noriega, Thomas R; Seol, Allen D; Robinson, Jon F; Bennett, Christopher L; Josifova, Dragana J; García-Verdugo, José Manuel; Katsanis, Nicholas; Hildebrandt, Friedhelm; Reiter, Jeremy F, A transition zone complex regulates mammalian ciliogenesis and ciliary membrane composition. *Nat. Genet.* **43**, 776–84 (2011).

12. Sulik, K; Dehart, D B; Iangaki, T; Carson, J L; Vrablic, T; Gesteland, K; Schoenwolf, G C, Morphogenesis of the murine node and notochordal plate. *Dev. Dyn.* **201**, 260–78 (1994).

13. Hu, Qicong; Milenkovic, Ljiljana; Jin, Hua; Scott, Matthew P; Nachury, Maxence V; Spiliotis, Elias T; Nelson, W James, A septin diffusion barrier at the base of the primary cilium maintains ciliary membrane protein distribution. *Science*. **329**, 436–9 (2010).

14. F. R. Garcia-Gonzalo, J. F. Reiter, Scoring a backstage pass: mechanisms of ciliogenesis and ciliary access. *J. Cell Biol.* **197**, 697–709 (2012).

15. T. Caspary, C. E. Larkins, K. V Anderson, The graded response to Sonic Hedgehog depends on cilia architecture. *Dev. Cell*. **12**, 767–78 (2007).

16. Aguilar, Andrea; Becker, Lars; Tedeschi, Thomas; Heller, Stefan; Iomini, Carlo; Nachury, Maxence V, A-tubulin K40 acetylation is required for contact inhibition of proliferation and cell-substrate adhesion. *Mol. Biol. Cell*. **25**, 1854–66 (2014).

17. Li, Yujie; Zhang, Qing; Wei, Qing; Zhang, Yuxia; Ling, Kun; Hu, Jinghua, SUMOylation of the small GTPase ARL-13 promotes ciliary targeting of sensory receptors. *J. Cell Biol.* **199**, 589–98 (2012).

18. A. Das, W. Guo, Rabs and the exocyst in ciliogenesis, tubulogenesis and beyond. *Trends Cell Biol.* **21**, 383–6 (2011).

19. M. C. Seabra, E. H. Mules, A. N. Hume, Rab GTPases, intracellular traffic and disease. *Trends Mol. Med.* **8**, 23–30 (2002).

20. H. Stenmark, Rab GTPases as coordinators of vesicle traffic. *Nat. Rev. Mol. Cell Biol.* **10**, 513–25 (2009).

21. J. S. Bonifacino, B. S. Glick, The mechanisms of vesicle budding and fusion. *Cell*. **116**, 153–66 (2004).

22. Barral, Duarte C; Garg, Salil; Casalou, Cristina; Watts, Gerald F M; Sandoval, José L; Ramalho, José S; Hsu, Victor W; Brenner, Michael B, Arl13b regulates endocytic recycling traffic. *Proc. Natl. Acad. Sci. U. S. A.* **109**, 21354–9 (2012).

23. Casalou, Cristina; Seixas, Cecília; Portelinha, Ana; Pintado, Petra; Barros, Mafalda; Ramalho, José S; Lopes, Susana S; Barral, Duarte C, Arl13b and the non-muscle myosin heavy chain IIA are required for circular dorsal ruffle formation and cell migration. *J. Cell Sci.* **127**, 2709–22 (2014).

24. Westlake, Christopher J; Baye, Lisa M; Nachury, Maxence V; Wright, Kevin J; Ervin, Karen E; Phu, Lilian; Chalouni, Cecile; Beck, John S; Kirkpatrick, Donald S; Slusarski, Diane C; Sheffield, Val C; Scheller, Richard H; Jackson, Peter K, Primary cilia membrane assembly is initiated by Rab11 and transport protein particle II (TRAPPII) complex-dependent trafficking of Rabin8 to the centrosome. *Proc. Natl. Acad. Sci. U. S. A.* **108**, 2759–64 (2011).

25. S. J. Scales, M. Gomez, T. E. Kreis, Coat proteins regulating membrane traffic. *Int. Rev. Cytol.* **195**, 67–144 (2000).

26. T. J. Pucadyil, S. L. Schmid, Conserved functions of membrane active GTPases in coated vesicle formation. *Science*. **325**, 1217–20 (2009).

27. J. R. C. Whyte, S. Munro, Vesicle tethering complexes in membrane traffic (2002).

28. J. E. Gerst, SNAREs and SNARE regulators in membrane fusion and exocytosis. *Cell. Mol. Life Sci.* **55**, 707–34 (1999).

29. J. G. Duman, J. G. Forte, What is the role of SNARE proteins in membrane fusion? *Am. J. Physiol. Cell Physiol.* **285**, C237–49 (2003).

30. Söllner, T; Whiteheart, S W; Brunner, M; Erdjument-Bromage, H; Geromanos, S; Tempst, P; Rothman, J E, SNAP receptors implicated in vesicle targeting and fusion. *Nature*. **362**, 318–24 (1993).

31. A. K. Gillingham, S. Munro, The Small G Proteins of the Arf Family and Their Regulators (2007), doi:10.1146/annurev.cellbio.23.090506.123209.

32. Y. Takai, T. Sasaki, T. Matozaki, Small GTP-binding proteins. *Physiol. Rev.* **81**, 153–208 (2001).

33. A. M. Rojas, G. Fuentes, A. Rausell, A. Valencia, The Ras protein superfamily: evolutionary tree and role of conserved amino acids. *J. Cell Biol.* **196**, 189–201 (2012).

34. K. Wennerberg, K. L. Rossman, C. J. Der, The Ras superfamily at a glance. *J. Cell Sci.* **118**, 843–6 (2005).

35. S. Pasqualato, L. Renault, J. Cherfils, Arf, Arl, Arp and Sar proteins: a family of GTP-binding proteins with a structural device for “front-back” communication. *EMBO Rep.* **3**, 1035–41 (2002).

36. S. R. Pfeffer, Structural clues to Rab GTPase functional diversity. *J. Biol. Chem.* **280**, 15485–8 (2005).

37. Q. Zhang, J. Hu, K. Ling, Molecular views of Arf-like small GTPases in cilia and ciliopathies. *Exp. Cell Res.* **319**, 2316–22 (2013).

38. Cuvillier, a; Redon, F; Antoine, J C; Chardin, P; DeVos, T; Merlin, G, LdARL-3A, a Leishmania promastigote-specific ADP-ribosylation factor-like protein, is essential for flagellum integrity. *J. Cell Sci.* **113 (Pt 1**, 2065–74 (2000).

39. Wiens, Cheryl J; Tong, Yufeng; Esmail, Muneer a; Oh, Edwin; Gerdes, Jantje M; Wang, Jihong; Tempel, Wolfram; Rattner, Jerome B; Katsanis, Nicholas; Park, Hee-Won; Leroux, Michel R, Bardet-Biedl syndrome-associated small GTPase ARL6 (BBS3) functions at or near the ciliary gate and modulates Wnt signaling. *J. Biol. Chem.* **285**, 16218–30 (2010).

40. Y. Li, K. Ling, J. Hu, The emerging role of Arf/Arl small GTPases in cilia and ciliopathies. *J. Cell. Biochem.* **113**, 2201–7 (2012).

41. Cantagrel, Vincent; Silhavy, Jennifer L; Bielas, Stephanie L; Swistun, Dominika; Marsh, Sarah E; Bertrand, Julien Y; Audollent, Sophie; Attié-Bitach, Tania; Holden, Kenton R; Dobyns, William B; Traver, David; Al-Gazali, Lihadh; Ali, Bassam R; Lindner, Tom H; Caspary, Tamara; Otto, Edgar a; Hildebrandt, Friedhelm; Glass, Ian a; Logan, Clare V; Johnson, Colin a; Bennett, Christopher; Brancati, Francesco; Valente, Enza Maria; Woods, C Geoffrey; Gleeson, Joseph G, Mutations in the cilia gene ARL13B lead to the classical form of Joubert syndrome. *Am. J. Hum. Genet.* **83**, 170–179 (2008).

42. N. a Duldulao, S. Lee, Z. Sun, Cilia localization is essential for in vivo functions of the Joubert syndrome protein Arl13b/Scorpion. *Development*. **136**, 4033–42 (2009).

43. M. Miertzschke, C. Koerner, M. Spoerner, A. Wittinghofer, Ac ce pte d Ma nu sc rip Ac ce pte d (2013).

44. Higginbotham, Holden; Guo, Jiami; Yokota, Yukako; Umberger, Nicole L; Su, Chen-Ying; Li, Jingjun; Verma, Nisha; Hirt, Joshua; Ghukasyan, Vladimir; Caspary, Tamara; Anton, E S, Arl13b-regulated cilia activities are essential for polarized radial glial scaffold formation. *Nat. Neurosci.* **16**, 1000–7 (2013).

45. Cevik, Sebiha; Hori, Yuji; Kaplan, Oktay I; Kida, Katarzyna; Toivenon, Tiina; Foley-Fisher, Christian; Cottell, David; Katada, Toshiaki; Kontani, Kenji; Blacque, Oliver E, Joubert syndrome Arl13b functions at ciliary membranes and stabilizes protein transport in Caenorhabditis elegans. *J. Cell Biol.* **188**, 953–969 (2010).

46. C. E. Larkins, G. D. G. Aviles, M. P. East, R. a Kahn, T. Caspary, Arl13b regulates ciliogenesis and the dynamic localization of Shh signaling proteins. *Mol. Biol. Cell*. **22**, 4694–703 (2011).

47. L. Hao, J. M. Scholey, Intraflagellar transport at a glance. *J. Cell Sci.* **122**, 889–92 (2009).

48. J. a. Follit, L. Li, Y. Vucica, G. J. Pazour, The cytoplasmic tail of fibrocystin contains a ciliary targeting sequence. *J. Cell Biol.* **188**, 21–28 (2010).

49. K. Madhivanan, R. C. Aguilar, Ciliopathies: The Trafficking Connection. *Traffic* (2014), doi:10.1111/tra.12195.

50. Y. Li, Q. Wei, Y. Zhang, K. Ling, J. Hu, The small GTPases ARL-13 and ARL-3 coordinate intraflagellar transport and ciliogenesis. *J. Cell Biol.* **189**, 1039–51 (2010).

51. J. A. Follit, R. A. Tuft, K. E. Fogarty, G. J. Pazour, The Intraflagellar Transport Protein IFT20 Is Associated with the Golgi Complex and Is Required for Cilia Assembly □. **17**, 3781–3792 (2006).

52. Follit, John a; San Agustin, Jovenal T; Xu, Fenghui; Jonassen, Julie a; Samtani, Rajeev; Lo, Cecilia W; Pazour, Gregory J, The Golgin GMAP210/TRIP11 anchors IFT20 to the Golgi complex. *PLoS Genet.* **4**, e1000315 (2008).

53. L. Milenkovic, M. P. Scott, R. Rohatgi, Lateral transport of Smoothened from the plasma membrane to the membrane of the cilium. *J. Cell Biol.* **187**, 365–74 (2009).

54. J. Wang, D. Deretic, Molecular complexes that direct rhodopsin transport to primary cilia. *Prog. Retin. Eye Res.* **38**, 1–19 (2014).

55. Nachury, Maxence V; Loktev, Alexander V; Zhang, Qihong; Westlake, Christopher J; Peränen, Johan; Merdes, Andreas; Slusarski, Diane C; Scheller, Richard H; Bazan, J Fernando; Sheffield, Val C; Jackson, Peter K, A core complex of BBS proteins cooperates with the GTPase Rab8 to promote ciliary membrane biogenesis. *Cell*. **129**, 1201–13 (2007).

56. Knödler, Andreas; Feng, Shanshan; Zhang, Jian; Zhang, Xiaoyu; Das, Amlan; Peränen, Johan; Guo, Wei, Coordination of Rab8 and Rab11 in primary ciliogenesis. *Proc. Natl. Acad. Sci. U. S. A.* **107**, 6346–51 (2010).

57. E. Seixas, M. Barros, M. C. Seabra, D. C. Barral, Rab and arf proteins in genetic diseases. *Traffic*. **14**, 871–85 (2013).

58. Dixon-Salazar, Tracy J; Silhavy, Jennifer L; Udpa, Nitin; Schroth, Jana; Bielas, Stephanie; Schaffer, Ashleigh E; Olvera, Jesus; Bafna, Vineet; Zaki, Maha S; Abdel-Salam, Ghada H; Mansour, Lobna a; Selim, Laila; Abdel-Hadi, Sawsan; Marzouki, Naima; Ben-Omran, Tawfeg; Al-Saana, Nouriya a; Sonmez, F Müjgan; Celep, Figen; Azam, Matloob; Hill, Kiley J; Collazo, Adrienne; Fenstermaker, Ali G; Novarino, Gaia; Akizu, Naiara; Garimella, Kiran V; Sougnez, Carrie; Russ, Carsten; Gabriel, Stacey B; Gleeson, Joseph G, Exome sequencing can improve diagnosis and alter patient management. *Sci. Transl. Med.* **4**, 138ra78 (2012).

59. X. Zuo, W. Guo, J. H. Lipschutz, The Exocyst Protein Sec10 Is Necessary for Primary Ciliogenesis and Cystogenesis In Vitro. **20**, 2522–2529 (2009).

60. Fogelgren, Ben; Lin, Shin-Yi; Zuo, Xiaofeng; Jaffe, Kimberly M; Park, Kwon Moo; Reichert, Ryan J; Bell, P Darwin; Burdine, Rebecca D; Lipschutz, Joshua H, The exocyst protein Sec10 interacts with Polycystin-2 and knockdown causes PKD-phenotypes. *PLoS Genet.* **7**, e1001361 (2011).

61. X.-M. Zhang, S. Ellis, A. Sriratana, C. a Mitchell, T. Rowe, Sec15 is an effector for the Rab11 GTPase in mammalian cells. *J. Biol. Chem.* **279**, 43027–34 (2004).

62. Feng, Shanshan; Knödler, Andreas; Ren, Jinqi; Zhang, Jian; Zhang, Xiaoyu; Hong, Yujuan; Huang, Shaohui; Peränen, Johan; Guo, Wei, A Rab8 guanine nucleotide exchange factor-effector interaction network regulates primary ciliogenesis. *J. Biol. Chem.* **287**, 15602–9 (2012).

63. Y. Jiu, C. Jin, Y. Liu, C. I. Holmberg, J. Jäntti, Exocyst subunits Exo70 and Exo84 cooperate with small GTPases to regulate behavior and endocytic trafficking in C. elegans. *PLoS One*. **7**, e32077 (2012).

64. Prigent, Magali; Dubois, Thierry; Raposo, Graça; Derrien, Valérie; Tenza, Danièle; Rossé, Carine; Camonis, Jacques; Chavrier, Philippe, ARF6 controls post-endocytic recycling through its downstream exocyst complex effector. *J. Cell Biol.* **163**, 1111–21 (2003).

65. Rogers, Katherine K; Wilson, Patricia D; Snyder, Richard W; Zhang, Xiaoyu; Guo, Wei; Burrow, Christopher R; Lipschutz, Joshua H, The exocyst localizes to the primary cilium in MDCK cells. *Biochem. Biophys. Res. Commun.* **319**, 138–43 (2004).

66. C. M. Babbey, R. L. Bacallao, K. W. Dunn, Rab10 associates with primary cilia and the exocyst complex in renal epithelial cells, 495–506 (2010).

67. M. Munson, P. Novick, The exocyst defrocked, a framework of rods revealed. *Nat. Struct. Mol. Biol.* **13**, 577–81 (2006).

68. W. Guo, D. Roth, C. Walch-Solimena, P. Novick, The exocyst is an effector for Sec4p, targeting secretory vesicles to sites of exocytosis. *EMBO J.* **18**, 1071–80 (1999).

69. Su, Xuefeng; Driscoll, Kaitlin; Yao, Gang; Raed, Anas; Wu, Maoqing; Beales, Philip L; Zhou, Jing, Bardet-Biedl syndrome proteins 1 and 3 regulate the ciliary trafficking of polycystic kidney disease 1 protein. *Hum. Mol. Genet.* **2**, 1–11 (2014).

70. N. Z. Gerges, D. S. Backos, C. N. Rupasinghe, M. R. Spaller, J. a Esteban, Dual role of the exocyst in AMPA receptor targeting and insertion into the postsynaptic membrane. *EMBO J.* **25**, 1623–34 (2006).

71. Boehlke, Christopher; Bashkurov, Mikhail; Buescher, Andrea; Krick, Theda; John, Anne-Katharina; Nitschke, Roland; Walz, Gerd; Kuehn, E Wolfgang, Differential role of Rab proteins in ciliary trafficking: Rab23 regulates smoothened levels. *J. Cell Sci.* **123**, 1460–7 (2010).

72. Sampaio, Pedro; Ferreira, Rita R: Guerrero, Adán; Pintado, Petra; Tavares, Bárbara; Amaro, Joana; Smith, Andrew a; Montenegro-Johnson, Thomas; Smith, David J; Lopes, Susana S, Left-right organizer flow dynamics: how much cilia activity reliably yields laterality? *Dev. Cell*. **29**, 716–28 (2014).

73. G. a Friedrich, J. D. Hildebrand, P. Soriano, The secretory protein Sec8 is required for paraxial mesoderm formation in the mouse. *Dev. Biol.* **192**, 364–74 (1997).

74. Zhao, Yuting; Liu, Jianglan; Yang, Changsong; Capraro, Benjamin R; Baumgart, Tobias; Bradley, Ryan P; Ramakrishnan, N; Xu, Xiaowei; Radhakrishnan, Ravi; Svitkina, Tatyana; Guo, Wei, Exo70 generates membrane curvature for morphogenesis and cell migration. *Dev. Cell*. **26**, 266–78 (2013).

Supplementary data

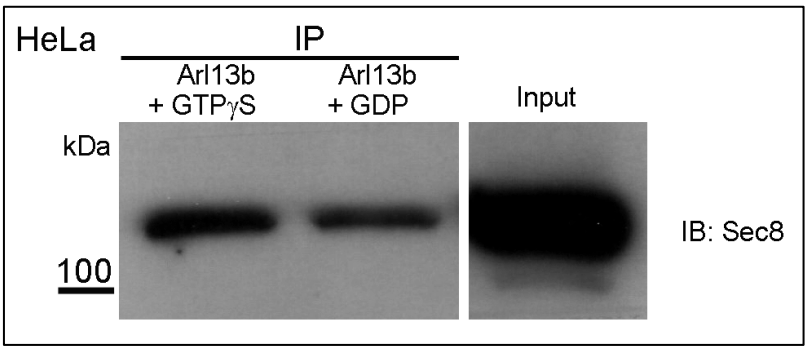

Supplementary Figure 1 - Sec8 is an Arl13b effector in non-ciliated cells. Total cell extracts from HeLa cells were immunoprecipitated with anti-Arl13b antibody in the presence of non-hydrolyzable GTP (GTPγS) or GDP. Immunoprecipitates were analyzed by SDS-PAGE and immunoblot with anti-Sec8 antibody.

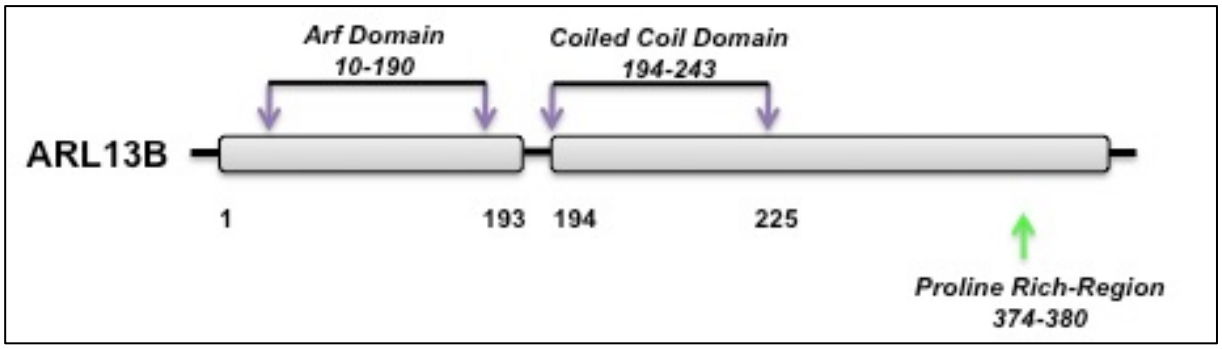

Supplementary Figure 2 - Schematic representation of the different domains of Arl13b. The Arf domain is responsible for the molecular exchanges between GTP and GDP, changing the protein between an inactive and active state to bind effectors. On the other hand coiled coil domain and proline rich-region are responsible for stabilize the protein conformation to allow the molecular switch between GTP and GDP. The mutant Arl13b [1-193]-EGFP contains only the Arf domain of the protein and the mutant Arl13b [194-428]-EGFP contains the coiled coil domain and the proline-rich region.

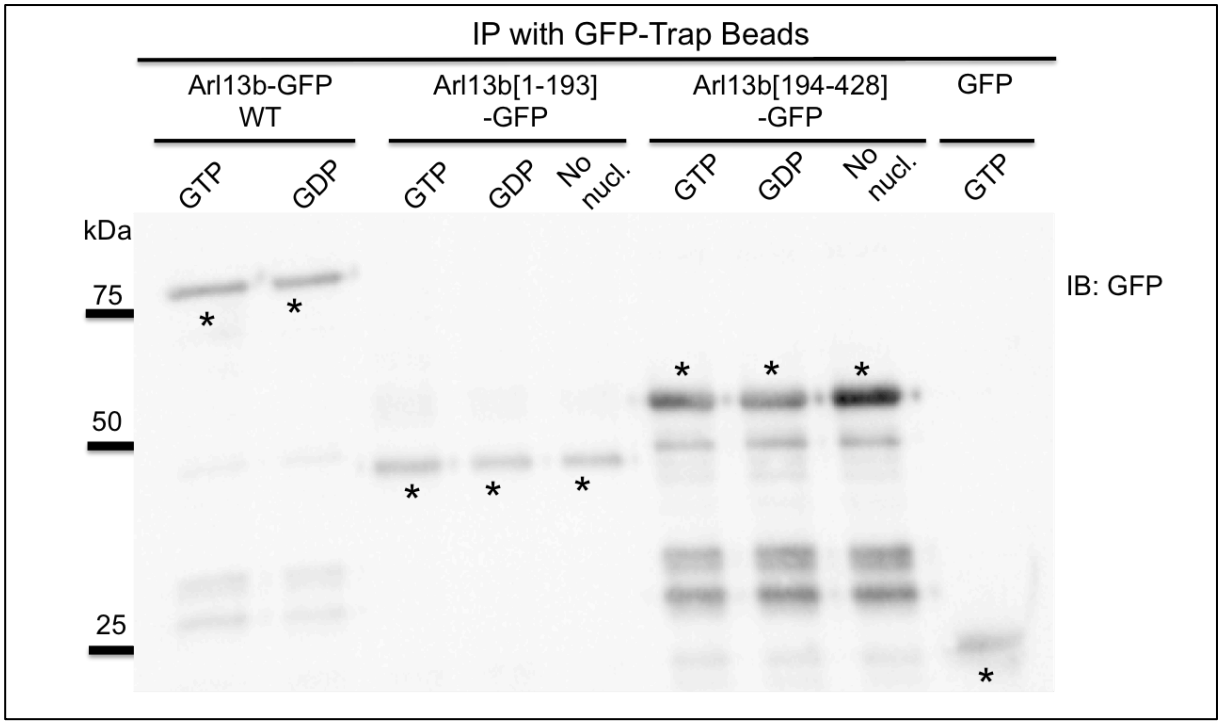

Supplementary Figure 3 – Arl13b-GFP pull-down efficiency. Cell lysates from HeLa cells (800 µg protein) overexpressing Arl13b-GFP full length, Arl13b[1-193]-GFP or Arl13b[194-428]-GFP were immunoprecipitated with GFP-trap beads to pull-down the Arl13b proteins tagged with GFP after pre incubation with GTPγS, or GDP or without any nucleotide (No Nucl.). Proteins in the immunoprecipitations were resolved by SDS-PAGE and immunblot with anti-GFP antibody. Asterisks (*) indicate the specific band for each construct.

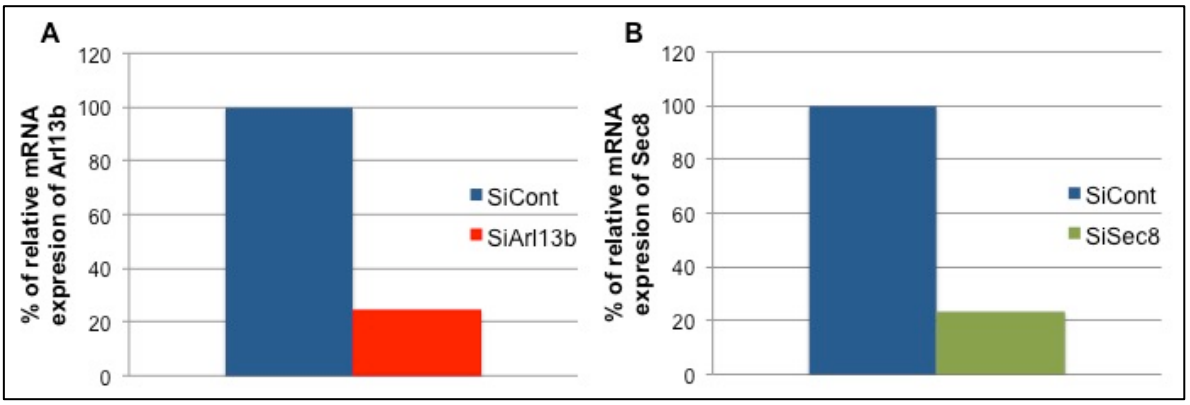

Supplementary Figure 4 – Quantification of silencing level by qRT-PCR. (A) Percentage of relative mRNA expression for Arl13b determined by qRT-PCR **(B)** Percentage of relative mRNA expression for Sec8 determined by qRT-PCR.